HOLOCENE SEDIMENTOLOGY OF OLD MAN LAKE, SOUTH EASTERN SOUTH AUSTRALIA.

This thesis is submitted in partial fulfilment for the Honours Degree of Bachelor of Science, Geology, University of Adelaide.

Antonio Mazzoleni B.Sc.
November 1993

CONTENTS

Abstract
Acknowledgements
List of Figures
List of Plates
List of Appendices

1. Introduction 1
2. Lake Setting 2
    2.1 Location, Morphology and Climate 2
    2.2 Geological Setting 2
        2.2.1 Regional Geology 2
        2.2.2 Local Geology 3
    2.3 Hydrology 3
        2.3.1 Regional Hydrology 3
        2.3.2 Local Hydrology 4
3. Water Chemistry 7
4. Sediment Facies 9
    4.1 Surface Facies 9
        4.1.1 Calcretised Sand Dune and Vegetated Dune Sand 9
        4.1.2 Lake-beach Sands and Associated Hardgrounds 10
        4.1.3 Fossil Thrombolite 11
            4.1.3.1 Bryozoa 22
            4.1.3.2 Green luminescence 23
    4.2 Stratigraphic Facies 24
        4.2.1 Stratigraphy of Core 1 (Lake Edge: North) 25
            4.2.1.1 Carbonate component grain description 25
            4.2.1.2 Siliciclastic component grain description 26
            4.2.1.3 Mineralogy 26
            4.2.1.4 Foraminifera 27
            4.2.1.5 Molluscs 27
            4.2.1.6 Bryozoa 28
            4.2.1.7 Hardgrounds 28
        4.2.2 Stratigraphy of Core 2 (Lake Centre) 29
            4.2.2.1 Carbonate component grain description 29
            4.2.2.2 Other properties 30
5. Organic Analysis of Old Man Lake Cores 33
    5.1 Rock-eval pyrolysis 33
    5.2 Gas Chromatography 37
        5.2.1 Middle Organic Unit 37
        5.2.2 Basal Organic Unit 38
6. Discussion 40
7. Conclusion 42
8. References 43

Abstract

Old Man Lake lies nestled within an inter-dunal hollow of the Robe Range, 13 km south of Robe. Three lithologically distinct Holocene sequences are observed in cored sections of the lake. A basal-dune sequence which is overlain by an estuarine sequence. Following the estuarine sequence is a lacustrine sequence. The sequence stratigraphy correlates to Holocene sea level change.

The occurrence of C_{25} highly branched isoprenoids (HBI) are characteristic of marine diatoms. Their observation in Old Man Lake sediments coupled with their appearance in Hamelin Pool (Shark Bay-Western Australia), may imply a restricted marine, rather than a marine, environment. Assuming a restricted marine environment, C_{25}-HBI may be used in the extrapolation of Holocene sea level changes, reflected in core sequence stratigraphy.

Fossil thrombolites characterise the eastern margin of Old Man Lake. The bryozoa, *C. aciculata* and green luminescing aragonitic gastropods are closely associated with the thrombolite. These three features may collectively imply a greater ground-water inflow operating in the past. Wetter conditions are known to have prevailed 6900 to 5000 years ago (Dodson 1974).

Acknowledgments

I gratefully acknowledge the following people for their assistance and support throughout my honours year.

My supervisors, Dr Yvonne Bone and Dr Vic Gostin, for their guidance and constructive comments.

Dr David McKirdy for his assistance in interpreting geochemical data.

Alan Brenchley for assistance in the acquisition of field data and the provision of transport.

Elizabeth Fontaine-Geary for her assistance in organic analyses.

Office and technical staff from the Adelaide University geology department.

Dr Quianyu Li and Graham Moss in the identification of foraminifera and other consulted staff members with whom I consulted throughout 1993.

Dr H. Veeh, Prof C.C von der Borch and the technical staff of Flinders University, in providing facilities for core storage and TOC analysis.

AMDEL for rock-eval pyrolysis and water analysis (Daryl Surkitt).

Paul, Kylie, Basim and Alison for their company during the year and constructive criticism

Kaye, for her eternal optimism and help in the outlay of my honours thesis.

Finally my Parents, for both their financial and emotional support throughout my scholastic journey, which began 21 years ago!!!

List of Figures

1. Locality Map.

2. Old Man Lake Surface Lithology.

3. Core 1 Stratigraphy and biota associations

List of Plates

Plate 1. Scenic view, looking north over Old Man Lake.

Plate 2. Northern beach of Old Man Lake.

Plate 3. Close up of gastropod cover from northern beach.

Plate 4. Eastern beach of Old Man Lake.

Plate 5. Hardground material of eastern beach.

Plate 6. Pit 2 hardground material, under cathodoluminescence.

Plate 7. Pit 2 hardground material, under cathodoluminescence, showing charcoal in contact with calcitic hardground.

Plate 8. Thrombolitic terrace from eastern margin of Old Man Lake.

Plate 9. Close up of clotted thrombolite.

Plate 10. Close up of semi-laminated thrombolite.

Plate 11. Thrombolite under cathodoluminescence, showing yellow-red foram luminescence

Plate 12. Thrombolite under cathodoluminescence, showing luminescence variation (green to yellow red) in gastropod.

Plate 13. Thrombolite under cathodoluminescence, showing isopachous calcite cement rimming an internal chamber of a gastropod.

Plate 14. Thrombolite under cathodoluminescence, showing emerald green luminescing layers.

Plate 15. Bryozoa (*C. aciculata*), encrusting thrombolite.

Plate 16. Location of bryozoa in thrombolite.

List of Appendices

Appendix I Analytical Techniques

A. TOC analysis.
B. Solvent extraction.
C. Column and gas chromatography.
D. X-ray diffraction analysis (XRD).
E. Cathodoluminescence analysis.
F. Rock-eval analysis.

Appendix II Gas Chromatography Results.

Appendix III Coring Methods.

Appendix IV Detailed Core Description.

Appendix V XRD Results.
A. Mineral percentages.
B. Trends.

Appendix VI Van Krevelen Diagrams.

1. Introduction

The Holocene stratigraphy of Old Man Lake differs in comparison to other lakes studied in south-eastern South Australia (eg von der Borch 1976, Warren 1988, Taylor 1975 and Rowe 1992). Complex carbonate mineral assemblages, such as magnesite, hydromagnesite, monohydrocalcite and dolomite, are common to many of the Coorong and Robe lakes further north but are absent in the stratigraphic record of Old Man Lake. A simple mineral assemblage characterises the stratigraphy of Old Man Lake. This simplicity allows for a clear understanding of Holocene sea level changes and its influence on local geology.

Differences in lateral lithologies are also useful in interpreting changes in depositional environments throughout the Holocene (eg Last 1992 and Taylor 1975). Old Man Lake displays a variation in surface lithology. Lake-beach deposits represent a current environment of deposition while a clotted thrombolitic terrace indicates a different depositional scenario operating in the past.

Hence both stratigraphy and surface lithologies are used in formulating the Holocene geology of Old Man Lake.

2. Lake Setting

2.1 Location, Morphology and Climate

Old Man Lake is approximately 300 km south of Adelaide and lies within the Little Dip Conservation Park (Fig 1). The lake is triangular in plan, has an area of ~ 3 ha and a maximum depth close to 3m (Fig 2). It is classified as one of the Robe-Beachport series of lake (Bayly and Williams 1966). Hence it experiences a similar climate, with an average annual rainfall of 50 to 60 cm and average temperatures ranging from 10°C in the coldest and wettest month of July to 15-20°C in the hottest and driest month of January (Bayly and Williams 1966). Wind direction is dominated by south westerlies blowing from the Southern Ocean (Fig 2). The water level of Old Man Lake fluctuates seasonally, with a significant increase being observed between the months of June and September. No permanent streams enter the lake, nor is there any connection of the lake to Lake Eliza or the Southern Ocean. Likely water sources are surface and sub surface runoff from surrounding dunes sands, direct input from rainfall and ground water.

2.2 Geological Setting

2.2.1 Regional Geology

Robe Range is the youngest of 20 emergent stranded calcareous sand barriers found parallel to the coast of south eastern South Australia (Sprigg 1952, Hossfeld 1950, von der Borch *et al.* 1980). The barriers cover a region 90 km wide by 400 km long (von der Borch *et al.* 1980). Each barrier represents a sea-level high stand which is directly related to glacio-eustatic oscillations that have occurred throughout the Quaternary (Sprigg 1952, Hossfeld 1950, von der Borch *et al.* 1980). The barriers are associated with lagoonal* and lacustrine deposits (von der Borch *et al.* 1980) and are formed on the high energy shorelines which follow a major transgression (Belperio and Cann 1990).

* The terms estuarine and lagoon have the same meaning in this thesis.

The strandlines increase in age away from the coast (Sprigg 1952, von der Borch 1976). Gentle regional up-warping of the coastal plain has occurred throughout the Quaternary and has been the dominant factor in preserving strandline features. The volcanic region of the far south east represents the centre of up warping (Sprigg 1952, Hossfeld 1950, von der Borch *et al.* 1980). Extensive calcrete development has also influenced preservation, commencing as soon as the sands become stabilised by vegetation (von der Borch *et al.* 1980).

2.2.2 Local Geology

Old Man Lake occupies a hollow within the Robe Range. Surrounding relief is low with dune ridges producing major topographic highs. The neighbouring Woakwine Range reaches a height of 45 m above sea-level (Burne and Ferguson 1983). Old Man Lake is enclosed from south east to north west by densely vegetated, unconsolidated sand (Fig 2). The sand is comparable, in age, to sand of the Younghusband Peninsula further north and to the Semaphore Sand of the Adelaide region. The remaining margin of the lake, away from the waters edge, consists of a lacustrine beach and surface hardgrounds, followed by 'fossil thrombolitic' terrace material (Y. Bone pers. comm. 1993). Calcretised dune sands form the final encompassing boundary (Fig 2).

2.3 Hydrology

2.3.1 Regional Hydrology

A regional carbonate aquifer underlies Old Man Lake, with a water flow directed westwards towards the coast (von der Borch *et al.* 1975, Burne and Ferguson 1983). The regional aquifer is referred to by Holmes and Waterhouse (1983) as the Upper Gambier Limestone. Water salinity of the aquifer is variable, ranging from 500 mg/L in the south east up to 5000 mg/L in the north west where precipitation is lower. A freshwater (Ghyben-Herzberg) lens, resting upon denser sea water, results in a salinity increase with depth (Holmes and Waterhouse 1983). A saline-freshwater interface between the Robe and Woakwine range exists. This interface currently dips easterly, with an angle ranging from 14° to 40° (Nelson 1972).

2.3.2 Local Hydrology

The local hydrology of Old Man Lake is poorly understood. The highly permeable dune sand may act as an unconfined aquifer and supply water to the lake when lake levels are low. Such a process has been described by Warren (1982). High permeability and therefore rapid infiltration would give little chance of evaporation, resulting in a very fresh water entering the lake (Nelson 1972).

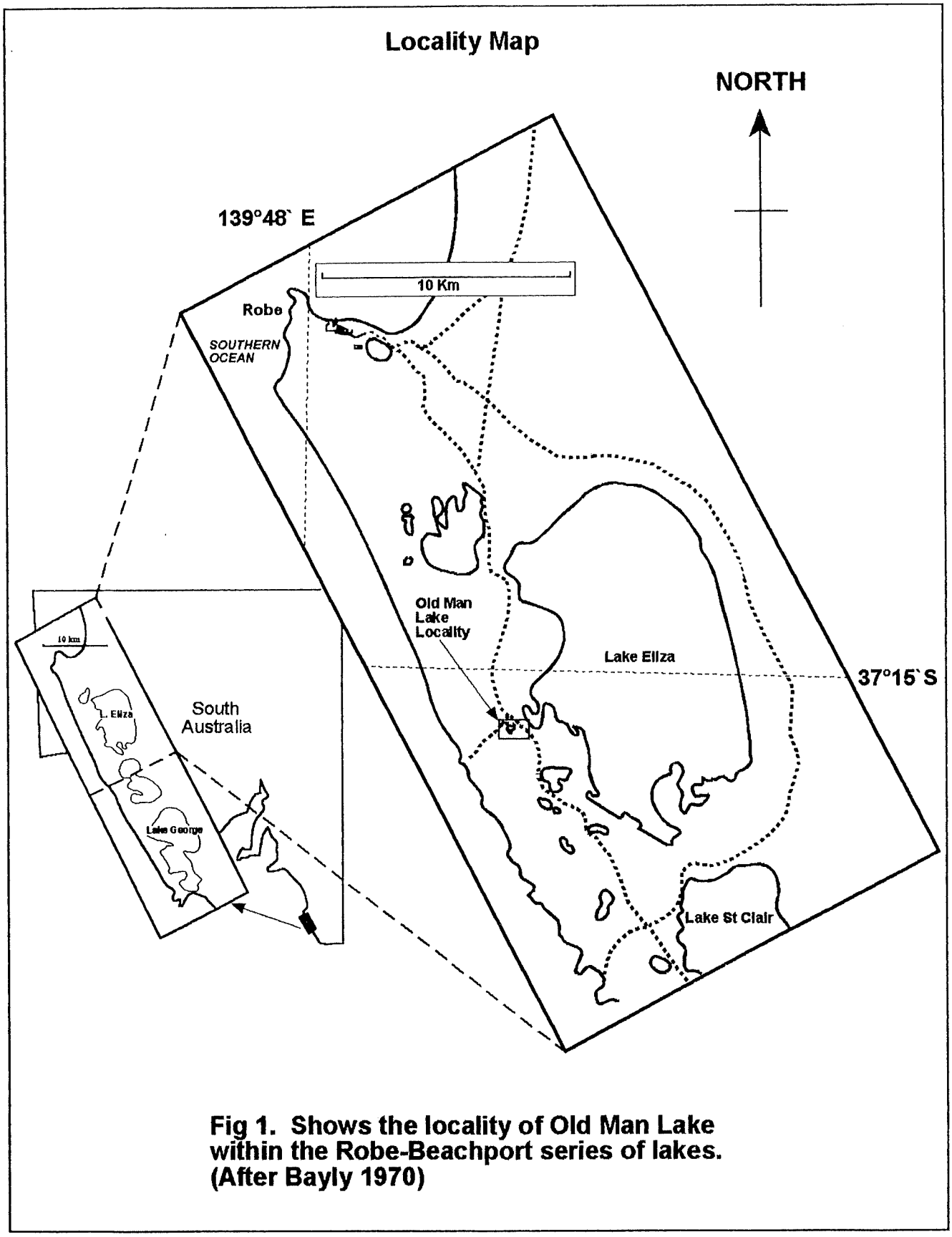

Fig 1. Shows the locality of Old Man Lake within the Robe-Beachport series of lakes. (After Bayly 1970)

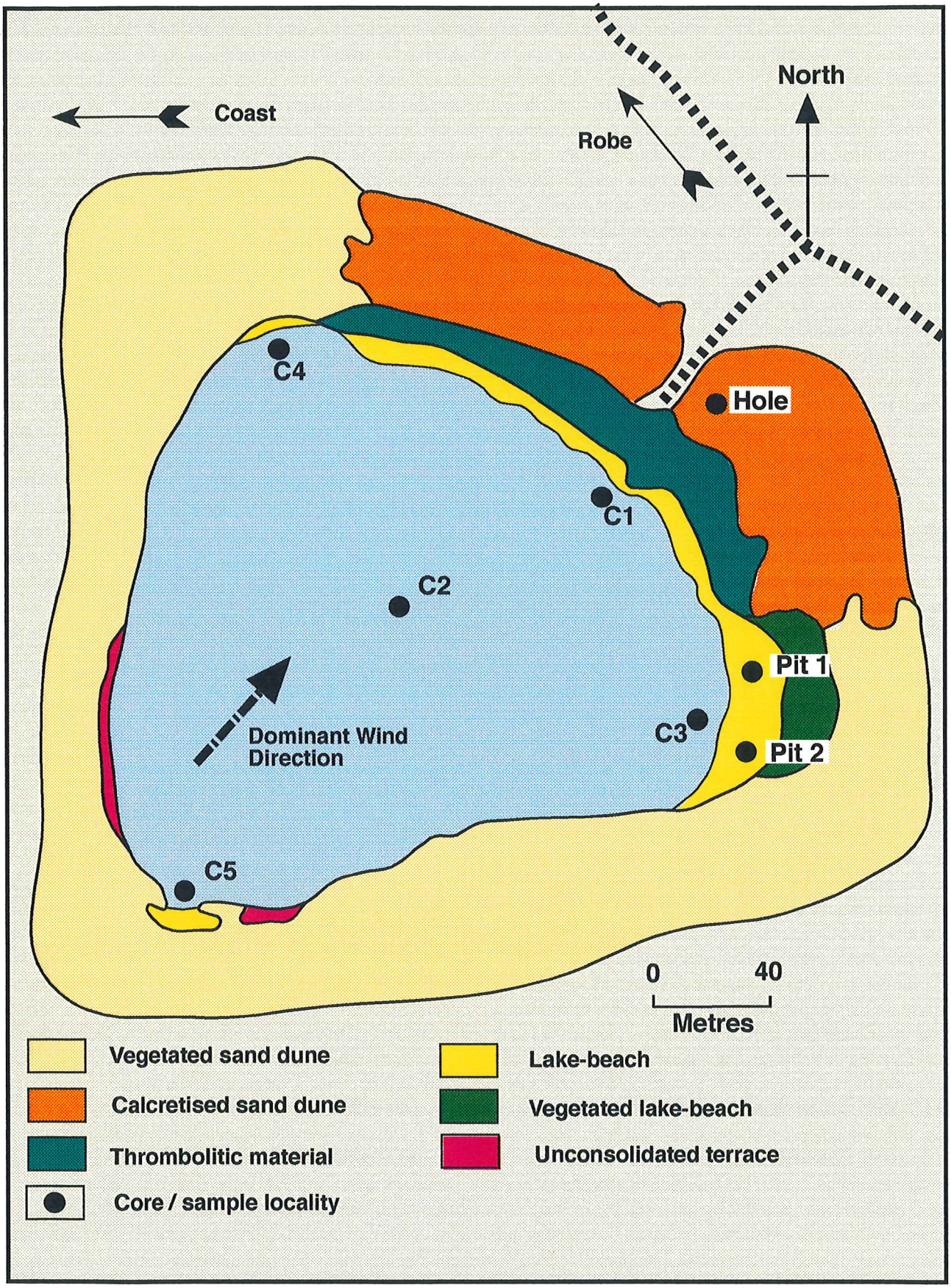

Fig 2. Old Man Lake local surface lithology

3. Water Chemistry

In May 1993 a water sample was collected from the centre of Old Man Lake, with water analysis undertaken at AMDEL (Thebarton, S.A.) laboratories the following August. Results of the analysis are summarised in Table 1.

The May water sample is saline, with analysis indicating high concentrations of sodium (11,695 mg/L) and chloride (20,917 mg/L) ions. The water has an ionic species ratio of $Na > Ca > Mg \geq K$ and $Cl > SO_4 > HCO_3$ and a salinity of 38277 ppm (or 38.28 ‰). Salinity is fractionally higher than that of normal marine water (33-38 ‰). On returning to the lake in September, salinity was much lower than in May and water level substantially higher. A decrease in salinity is a result of increased direct precipitation and sub-surface water in-flow from surrounding dunes, caused by higher rainfalls occurring during the winter months. The pH of lake water is 7.7 (near neutral), while conductivity is approximately 54600 μScm^{-1} at 25°C. Measurements taken in the field give an average pH reading of 7.48, which is slightly less alkaline than the laboratory measurement. A striking feature of the water analysis was the ammonia concentration of 0.78 mg/L. Normal concentrations of aqueous NH_3 are usually less than 0.1 mg/L (D.Surkitt, AMDEL, pers. comm. 1993).

"Putrefaction of organic material in a lime-rich solution creates carbon dioxide and ammonia. The carbon dioxide causes the lime to be dissolved which forms ammonium carbonate in solution. The ammonium carbonate breaks down by evaporation or is broken down by the organic action of moulds, bacteria and algae to form a carbonate precipitate of sparry, amorphous, and crystalline calcite and aragonite" (H.J McCunn, page 150, 1972). Such a process may be active in Old Man Lake and hence provide an explanation for the high levels of ammonia observed.

Water Analysis: Old Man Lake

Ionic Species	Symbol	mg/L	**me/L
Cations			
Calcium	Ca	1740	86.83
Magnesium	Mg	495	40.74
Sodium	Na	11695	508.7
Potassium	K	420	10.74
Anions			
Hydroxide	OH	0	0
Carbonate	CO3	0	0
Bicarbonate	HCO3	310.7	5.09
Sulphate	SO4	2855	59.44
Chloride	Cl	20917	589.2
Nitrate	NO3	< 0.1	-
Ammonia (non-ionic)	NH3	0.78	-

Totals and Balance	%	**me/L
Cations		647
Anions		653.7
Difference		6.73
Sum		1300.75
***Ion Balance	0.52%	
Sodium/Total Cation Ratio	78.60%	

Other Measurements	
Reaction pH	7.7
Conductivity (micro S/cm @ 25°C)	54600
Resistivity (Ohm M @25°C	0.18

Derived Data	mg/L
Total Dissolved Solids	
A. Based on *E.C	45736
B. Calculated (HCO3=CO3)	38277
Total Hardness	6381
Carbonate Hardness	248
Non-Carbonate Hardness	6132
Total Alkalinity (each as CaCO3)	248

***E.C is a laboratory formula**
****me/L=mg/L divided by Atomic Mass of Ion.**
*****Ion Balance = Difference x 100/Sum**

Method WAT 2
Job number 3AD2917
Done at AMDEL laboratories Thebarton, Adelaide, South australia

mg/L=milligrams per litre
me/L=milliequivs per litre

Salinity
Salinity in this circumstance is considered to be equivalent to the total dissolved solids in part B of derived data.
Salinity (ppm)= 38277 and therefore= 38.28 ‰

Table 1. Water analysis of Old Man Lake. Sampled May 1993.

4. Sediment Facies

Changes in both surface (lateral) and stratigraphic (vertical) facies are observed within the study area. Lateral facies descriptions are based upon surface samples collected from the north, east and southern sides of the lake, while five cored sections provide information on lake stratigraphy. Four cores were taken from the lake edge (C1, C2, C3 and C4) and one from the lake centre (C2) (Fig 2). Coring methods are described in Appendix III. A two metre deep hole supplemented the cores. The hole is located in the picnic area of Old Man Lake, approximately 35 m north-east from C1 (Fig 2).

4.1 Surface Facies

Many different lithologies constitute the modern sedimentary surface facies of Old Man Lake (Fig 2). They include:

- Calcretised sand dune and vegetated dune sand.
- Lake-beach and associated hardground features.
- Lithified porous carbonate material (fossil thrombolitic material)

4.1.1 Calcretised Sand Dune and Vegetated Dune Sand

Calcretised dune sand was collected from the dune range bordering the eastern margin of the lake. The calcretised sand is composed of well sorted, angular to sub-angular sand size grains. Some grains are frosted, indicating an aeolian input. Calcretised sand varies in mineralogy. X-ray diffraction (XRD) analysis (Appendix I) revealed calcrete sand samples composed of quartz (35%), aragonite (34%) and calcite (31%) whereas 100% calcite samples are also observed. Variations in mineralogy may indicate different maturity levels with respect to calcrete formation and/or possibly a change in source material. Calcareous grains of both calcretes consisted of mollusc and other carbonate skeletal fragments.

Poorly consolidated sand stabilised by a variety of flora encompasses most of Old Man Lake (Fig 2). The texture of the sand is identical to its calcretised counterpart. Mineralogy of the sand is quartz (31%), aragonite (37%) and calcite (32%).

4.1.2 Lake-beach Sands and Associated Hardgrounds

Lake-beach sediments are observed along the northern and eastern margins of Old Man Lake (Plate 1 and Fig 2). They are only exposed during times of low water level.

The lake-beach facies varies laterally from east to north. Northern sediment is strongly dominated by aragonitic gastropods (Plate 2 & 3), Contrasting with the northern lake-beach, the eastern lake-beach sediment is composed of a well sorted silt (Plate 4) and is lacking in coarse gastropod component.

Calcareous pieces of hardground material cover the eastern beach of Old Man Lake (Plate 5). The shape of the hardground varies, with some pieces having a tabular morphology whereas others were jagged and lacked any distinguishable shape. X-ray diffraction (XRD) and cathodoluminescence (CL) analyses (Appendix I) reveal a calcite mineralogy with minor amounts of quartz . The hardground is classified as a cementstone according to Wright's terminology (1992).

Similar hardground material is also found in two pits dug approximately 15 metres from the water line (Fig 2). Calcite hardground layers are found in Pit 1, at 12 and 30 cm depth and in Pit 2, at depths of 10 cm and 24 cm. Plate 6 shows the red-orange luminescing, calcite hardground of pit 2 (24 cm) under CL. A charcoal component is found in the 24cm deep hardground of pit 2, which may indicate a human presence in the past, or a previous occurrence of forest fires. The contact of speckled black charcoal with neighbouring red-orange calcite cement can be observed in Plate 7.

A (3.0 mol % $MgCO_3$) low-Mg calcite (LMC) hardground is found at the sediment-water interface near the northern beach. It possessed a thin, brittle, indurated fabric.

Hardground material is produced by carbon dioxide degassing from lime-rich solutions. Seasonal groundwater incursions occurring at a shallow depth may, when on reaching the sediment-water interface, decompress (lower ρ_{CO2}) and hence become supersaturated with respect to a carbonate phase (Last 1992, James and Choquette 1990). That is removing CO_2 from equation shifts the reaction to the left which favours the formation of a mineral phase.

$$CaCO_3 + H_2O + CO_2 = Ca^{+2} + 2HCO_3^{-2}$$

Equation 1. Simple reaction between carbonate mineral phase and meteoric water. (James and Choquette 1990)

Depending on water chemistry, different carbonate phases will precipitate according to their solubility products. In the case of Old Man Lake, which is a surface expression of the water table, both calcium and carbonate/bi-carbonate concentrations are high while magnesium concentrations are low (Table 2). As a consequence, a potential for calcite hardground formation through degassing exists. (Mg being low in concentration inhibits the formation of other carbonates phases eg dolomite, magnesium calcite and monohydrocalcite.) Degassing may also explain the occurrence of hardgrounds at depth.

4.1.3 Fossil Thrombolite

A thrombolite is a descriptive term used to describe the internal structure of calcareous microbialites. Microbialites are organosedimentary deposits accreted by benthic microbial communities. Thrombolites are recognised by their distinctive clotted fabric. The clots (mesoclots) form a rigid framework which is produced by *in situ* microbial calcification, rather than by trapping and binding of detrital sediment. Binding and trapping generally leads to stromatolite formation (Kennard and James 1986). A lack of trapping and binding may indicate a rapid rate of calcification (Burne and Moore 1987).

Individual clots may form from coccoid-dominated and/or filamentous microbial communities. The cyanobacterium, *Scytonema*, is considered to be an important filamentous calcifer in thrombolites. It

can tolerate high salinities in excess of 65 ‰, but commonly prefers low to normal salinities. Strong evidence suggests that thrombolites once accommodated abundant and diverse skeletal and soft-bodied metazoan fauna (Burne and Moore 1987).

Microbialites are currently forming in Lake Clifton, Western Australia. Lake Clifton occupies a coastal plain depression, bounded to the east by Holocene Dunes. The salinity of Lake Clifton is low, but varies seasonally from 17 to 30 ‰. "Pustular doughnut" microbial lithoherms, possessing a thrombolitic fabric are observed along the eastern shoreline in close association with a zone of ground-water discharge (Moore *et al.* 1984). Ground-water salinity is low (~ 2 ‰), rich in calcium and bicarbonate ions, and favours thrombolite formation by:

i) Minimising the effects of exposure (desiccation) during periods of low water level (dry periods).

ii) Lowering salinity and therefore producing conditions favourable for the growth of *Scytonema*, the main constructive organism of Lake Clifton thrombolites.

iii) Makes available Ca^{+2}, CO_3^{-2} and HCO_3^{-1}; ions that are required in a calcification process

(Moore 1987)

The fossil thrombolites of Old Man Lake are confined to the eastern margin and form the main component of the lake-terrace (Plate 8 and Fig 2). An oyster bed belonging to the estuarine sequence appears to directly underlie the thrombolite. The internal structure of the thrombolite is predominantly clotted to tuffaceous (Plate 9), however semi-laminated (stromatolitic ?) structures are also observed (Plate 10). The clotted thrombolite is similar to "pustular doughnut" thrombolite found in Lake Clifton Western Australia (Moore 1987, Burne and Moore 1987, Sprigg and Bone 1993) and beachrock found in Lake Fellmongery (Taylor 1975, Rowe 1992).

Contained within the thrombolitic material are ostracods, various types of worm tubes, bryozoa, gastropods, foraminifera and bivalves. Such diverse biota associations are common to mesoclots, the primary building block and diagnostic feature of thrombolites. Unconsolidated sediment containing ostracod and gastropod shells are observed accumulating between an irregular framework of thrombolite mesoclots from Lake Clifton (Burne and Moore 1987).

Old Man Lake thrombolite consists of biogenic elements (skeletal fragments) bound by a carbonate cement. The carbonate cement is composed of (6 mol% $MgCO_3$) Mg-calcite (IMC). High (12 mol% $MgCO_3$) Mg-calcite is also present, but in minor amounts. Biogenic grains are found to range in composition.

Foraminifera appear yellow-red under CL (Plate 11), indicating a calcitic composition. Gastropods show a variation in mineralogy within individual skeletal grains, ranging from an aragonite which luminesces green under CL, through to a yellow calcite (Plate 12 & 13). (XRD analysis confirms an aragonite mineralogy for the gastropod.)

Isopachous, crystalline, calcite cement can be detected rimming an internal chamber of some gastropods (Plate 13). However calcite generally occurs as an infill in most gastropod chambers and is usually deficient in a crystalline texture.

Layered structures within the thrombolite also exhibited green luminescence under CL (Plate 14). Bryozoa, encrusting the thrombolite, is composed of (8 mol% $MgCO_3$) Mg-calcite (IMC). CL analysis was not performed on the bryozoa due to an insufficient amount of sample.

Plate 1. View looking north over Old Man Lake

Plate 2. Nothern beach showing gastropod rich cover.

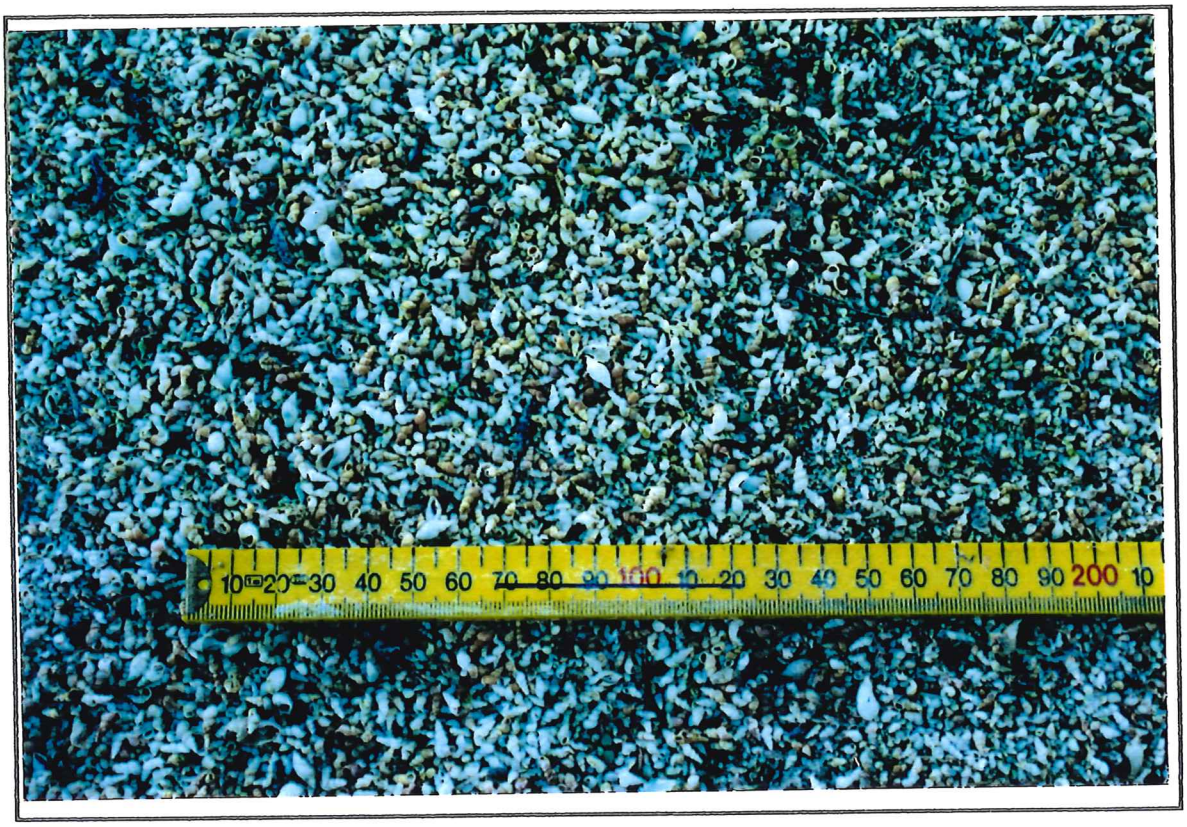

Plate 3. Close up of gastropod rich cover from northern beach (Plate 2)

Plate 4. Eastern beach of Old Man Lake. (Pit 1 is indicated by a hat on a shovel, left of picture)

Plate 5. Hardground material of eastern beach.

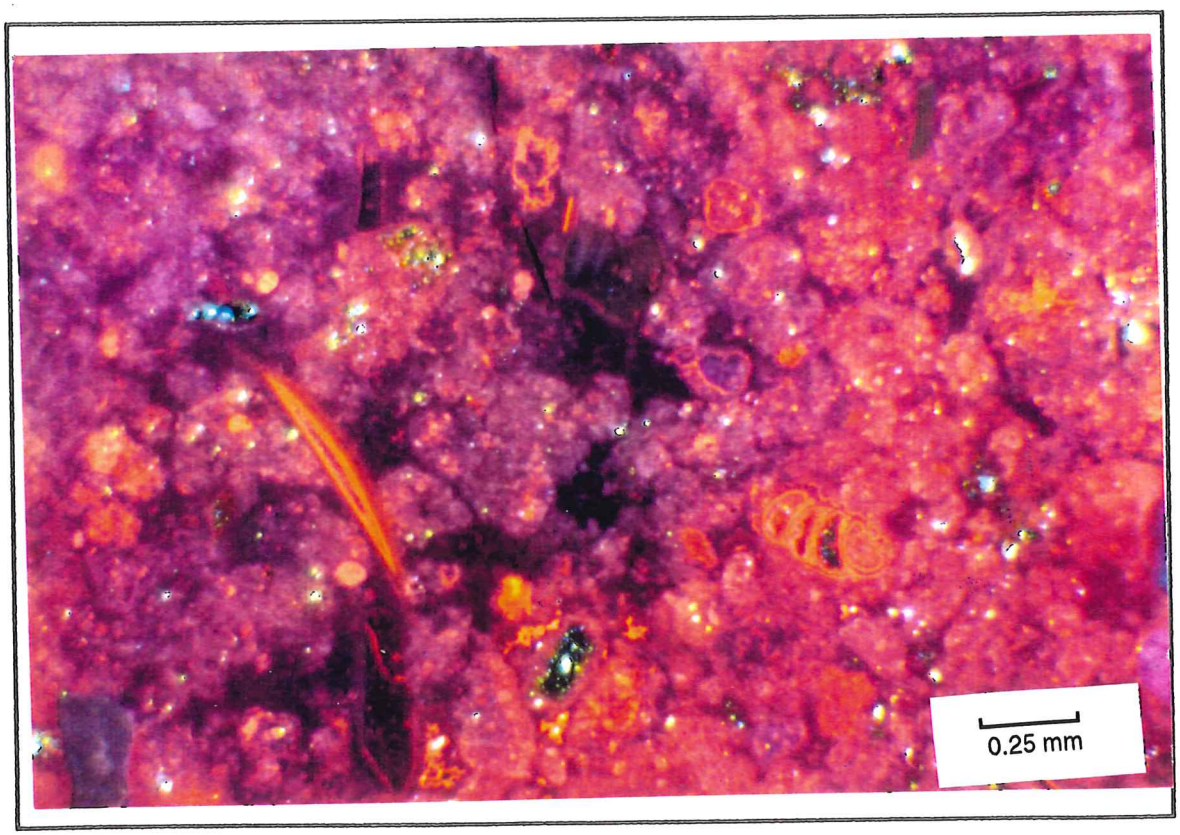

Plate 6. Hardground material from pit 2 (24 cm depth) under CL.

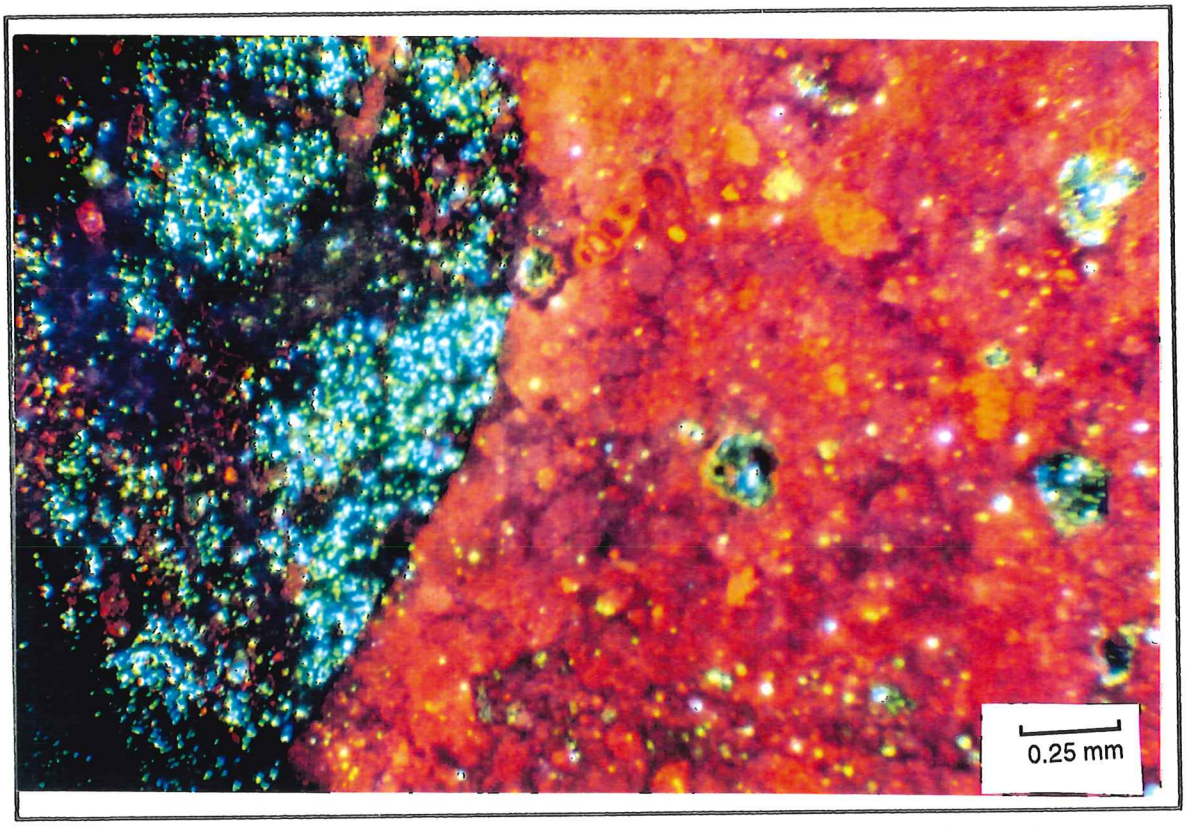

Plate 7. Charcoal (speckled black) in contact with red luminescing calcitic hardground material from pit 2 at 24cm depth. Sample under CL.

Plate 8. Thrombolitic terrace material from eastern margin of Old Man Lake.

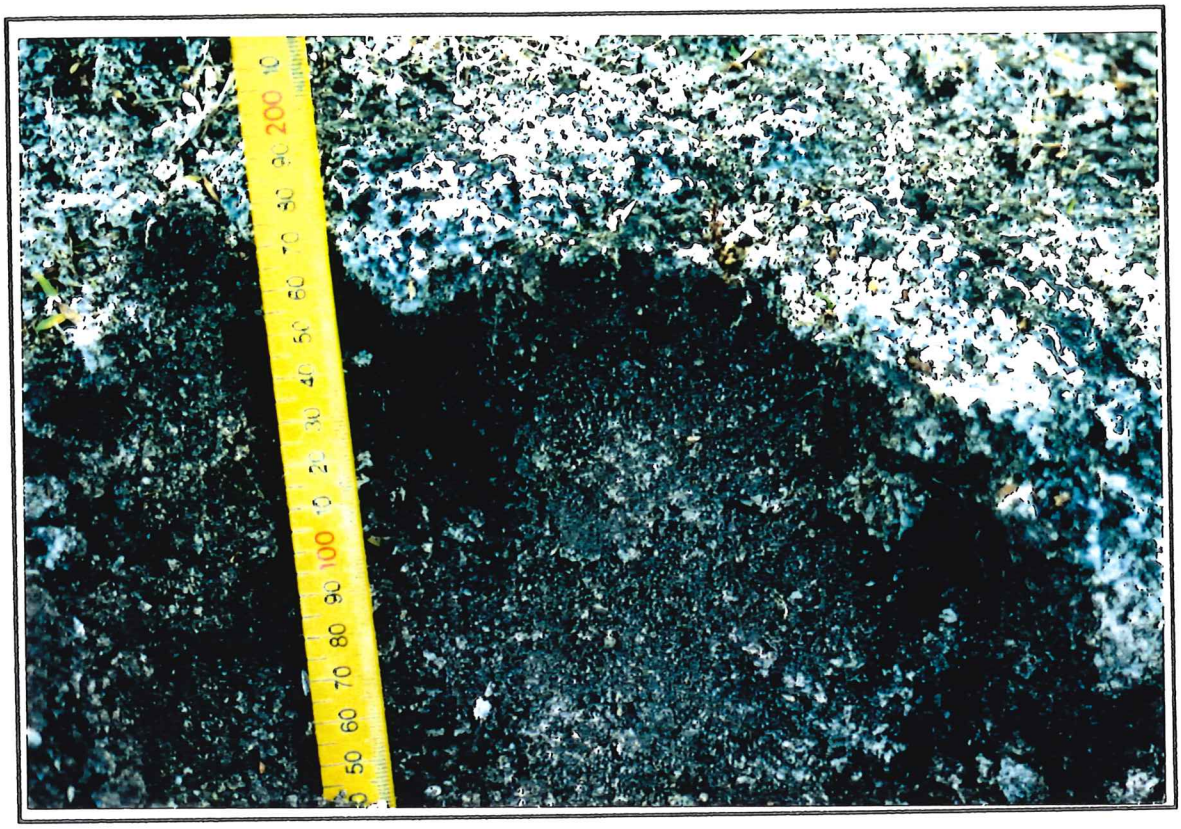

Plate 9. Close up clotted thrombolite. Weathered sample.

Plate 10. Semi-laminated thrombolite (possibly stromatolitic).
Note divisions on ruler in centimetres.

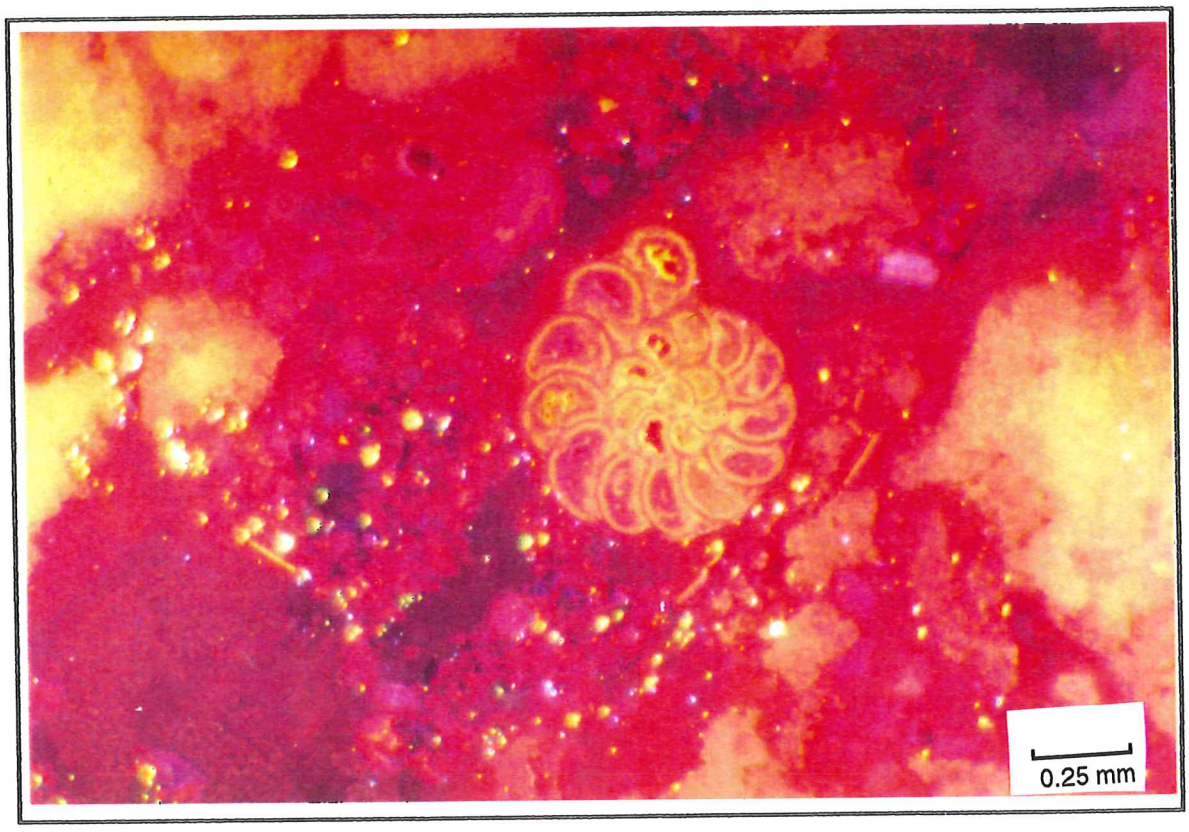

Plate 11. Thrombolite under CL. Note yellow-red, calcitic foram in centre of picture.

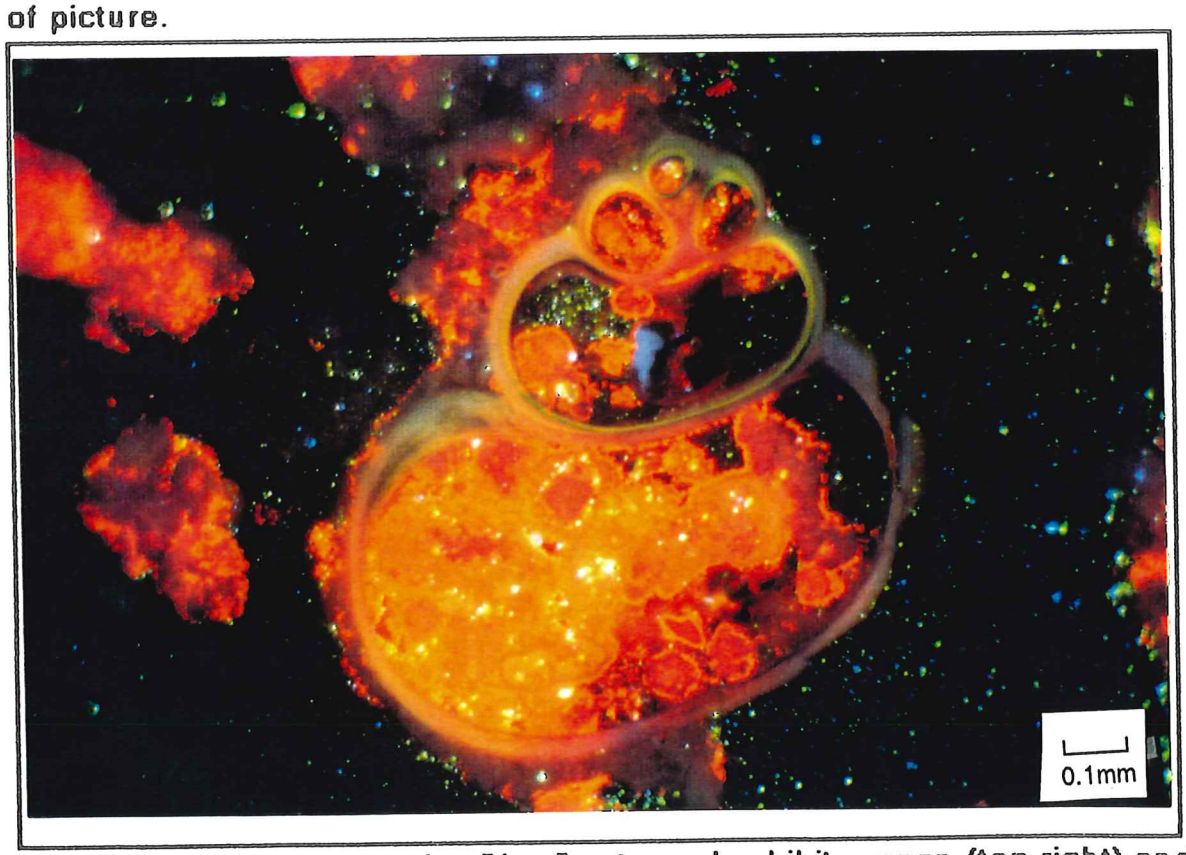

Plate 12. Thrombolite under CL. Gastropod exhibits green (top right) and yellow-green (most of gastropod shell) luminescence, which is characteristic of aragonite. Red-orange luminescing calcite occupies the bottom left and internal chambers of the gastropod).

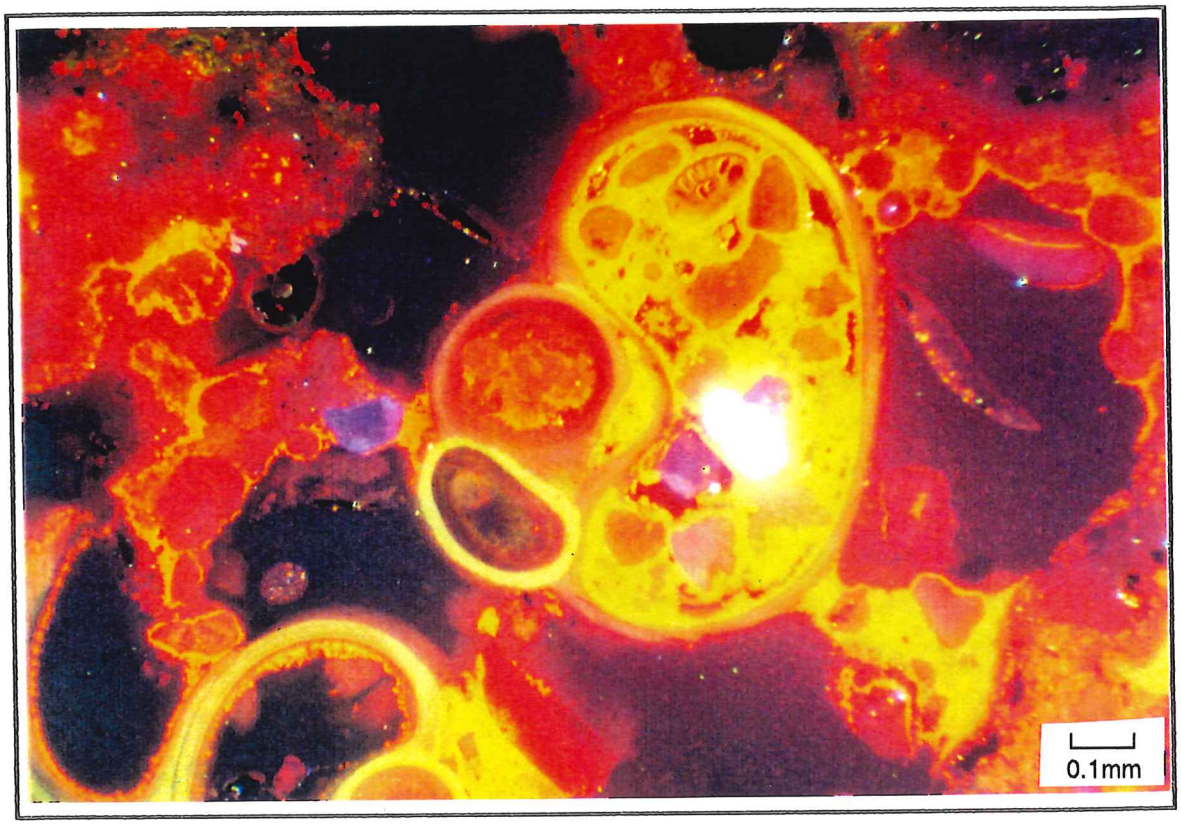

Plate 13. Thrombolite under CL. Gastropod luminesces yellow-green aragonite) to orange-red (calcite). Note isopachus calcitic crystalline cement rimming internal chamber of gastropod in bottom left hand corner.

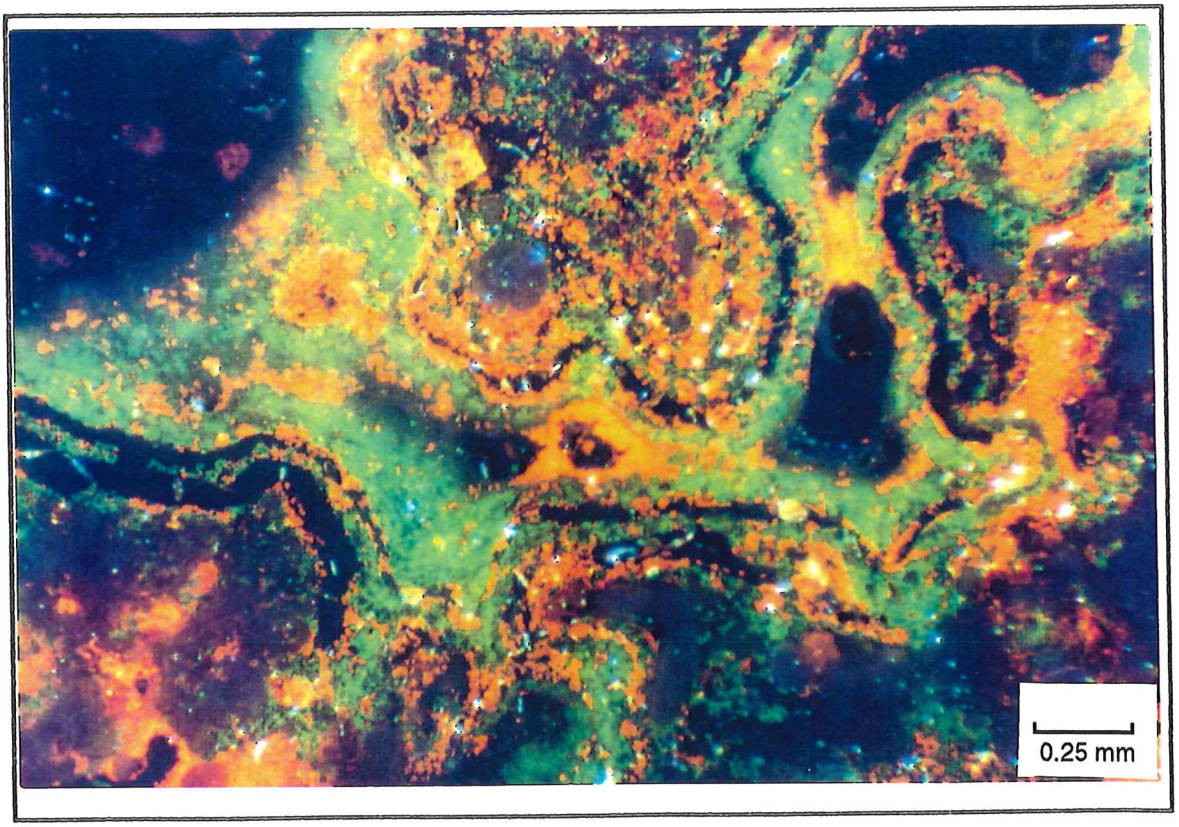

Plate 14. Thrombolite under CL. Shows the emerald-green (aragonite) luminescing layers.

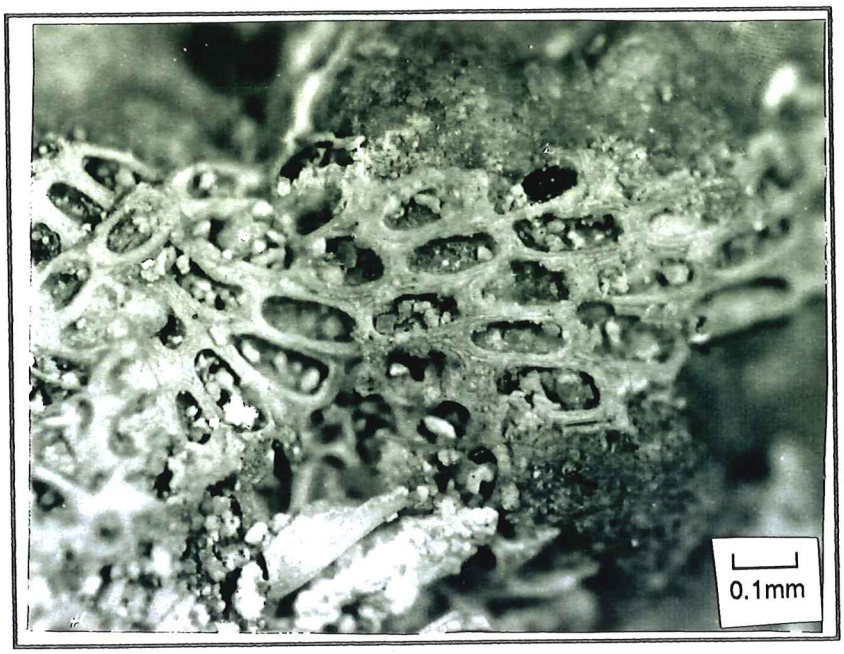

Plate 15. Bryozoa *C. aciculata*. Under white light.

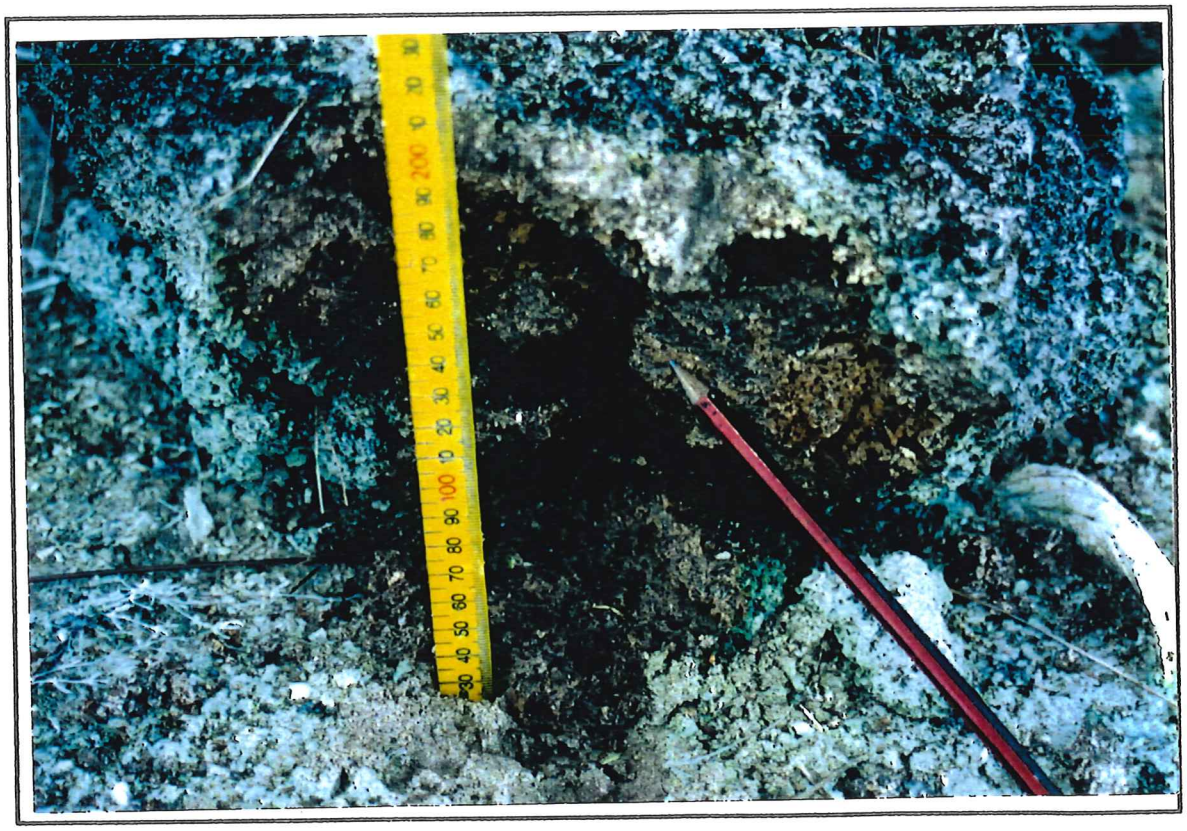

Plate 16. Throbolite in which bryozoa was found (indicated by pencil)

4.1.3.1 Bryozoa

Uni-laminar colonies of the bryozoa, *Conopeum aciculata* (MacGillivray 1891, Sprigg and Bone 1993), were found within the "Pustular doughnut" thrombolitic terrace material of Old Man Lake (Plate 15 and 16). Uni-laminar *C. aciculata* is presently living in Old Man Lake. It was found as a small colony, encrusting a sub-recent oyster shell.

Water depth and salinity are controlling factors in the growth of the bryozoa, *C. aciculata.* Bryozoa growth is favoured in a hyposaline, sub-tidal environment, or an environment which is not prone to long periods of exposure and desiccation (Bone and Wass 1990).

C. aciculata is considered to be an opportunistic fauna, which is able to capitalise on slight changes in previously unfavourable environments (Bone 1991).

C. aciculata was previously reported in the Coorong lagoon of south-eastern South Australia (Bone and Wass 1990, Bone 1991, Sprigg and Bone 1993). Both Sub-recent (760 years **BP**) and Recent *C. aciculata*-serpulid buildups were observed in the Coorong lagoon. Their growth was multiserial and multilaminar (Sprigg and Bone 1993), with $\delta^{18}O$ enrichment indicating a Coorong salinity marginally higher than normal seawater. Today, during periods of high evaporation, Coorong salinities may range from a maximum of 50 ‰ in the north through to 60‰ in the south. In winter the salinity approaches that of normal seawater (36‰) (Bone and Wass 1990).

C. aciculata currently lives within the Coorong lagoon. Growth is unilaminar with buildups occurring episodically. Each episode reflects a decrease in salinity and hence the propagation of bryozoa growth. Bone (1991) observed a drastic increase in *C. aciculata* buildups at Magrath Flat (Coorong) during the spring of 1989. Prior to 1989, bryozoa colonies had been sparsely distributed throughout a stressed marine environment (Bone and Wass 1990). The population explosion of *C. aciculata* was explained by an atypically wet winter experienced by the Coorong region. Unusually high rainfall resulted in the lowering

of salinity throughout the Coorong lagoon and resulted in the population explosion of *C. aciculata* (Bone 1991).

A close association between thrombolite and *C. aciculata* is also observed in Lake Clifton, Western Australia. The bryozoa is found to be growing over and throughout thrombolite (Sprigg and Bone 1993).

4.1.3.2 Green luminescence

Manganese (Mn) is an important trace-element activator in carbonate rocks (Sommer 1972). It promotes, through the excitation and subsequent relaxation of electrons, an active luminescence, which is dependent upon a variety of parameters. The parameters include:

- *Orbital transition states* : Yellow-green luminescence is characteristic of aragonite, and is thought to be caused by the transition of electrons from an un-split electronic T_{1g} state (an excited state) to the ^6S state (ground state) within the manganese ion, Mn (+2).

- *Mn oxidation state* : Valence state of the activator ion may influence the wavelength of the luminescence. Manganese in a (+2) oxidation state produces a broad structureless red or green emission. Mn (+4) is characterised by a emission in the red narrow-band emission (Kröger 1948, Sommer 1972). Average valencies of (+2) cause a green and yellow luminescence while orange and red luminescence is caused by a mixture of Mn valencies, some with +2 and others with valencies greater than +2 (Osiko and Maksimova 1960, Sommer 1972).

- *Mn coordination* : Green emitting Mn arises when the cation is in 4-fold coordination with oxygen while 6-fold coordination of the Mn activator is responsible for the red emission (Linwood and Weyl 1942, Sommer 1972).

- *Lattice positioning of Mn ions*: Mn(+2) occupying interstitial positions of spar produces green luminescence. Mn(+2) replacing Ca(+2) in the aragonite lattice results in an orange-red emission (Barsanov and Sarsembaeva 1962, Sommer 1972).

Marine aragonite can be distinguished from freshwater aragonite in that it shows little or no luminescence compared to freshwater aragonite which luminesces yellow-green. Luminescent properties of both freshwater and marine aragonites are explained by Mn concentration differences. Lakes and rivers (freshwater Mn sources) contain sufficient amounts of Mn, so that any aragonite precipitating is capable of luminescing. This is not apparent for marine waters, where Mn concentrations are too low and hence aragonite formed under such conditions will not luminesce. Maximum Mn(+2) activated luminescence of aragonite occurs at Mn concentrations of 500 ppm, though concentrations of 1000 ppm have also been reported as giving a maximum luminescence (Sommer 1972)

Green luminescence is rarely reported. A reason for this could be that most aragonite occurrences are usually marine in origin. However it is more likely a result of little CL work being performed on lacustrine carbonate rocks.

The occurrence of bryozoa (*C. aciculata*), together with the luminescent properties of aragonite, is unique. Green aragonite is rarely reported for lacustrine carbonate rocks, whilst *C. aciculata* has not previously been reported from any of the Robe-Beachport series of lakes.

The distribution of fossil thrombolites in Old Man Lake may possibly indicate an environment similar to that of Lake Clifton today (Sprigg and Bone 1993). The association of thrombolites within a ground-water discharge zone is further supported by the appearance of green luminescing freshwater aragonite, which is displayed by both gastropod and layered structures. The appearance of bryozoa *C. aciculata* within the thrombolites of Old Man Lake provides additional evidence for such an association.

4.2 Stratigraphic Facies

Three lake edge cores C3, C4 and C5, were sampled at closely spaced intervals. A mineral assemblage of aragonite, calcite and quartz was detected using X-ray diffraction methods (Appendix I). Relative

changes in each mineral component occurred with increasing, depth producing stratigraphic trends (Appendix V). A high degree of correlation was observed between the three cores. This good correlation justified extrapolating the trend to core 1 (C1), located on the northern edge of the lake.

Core 1 was collected using a vibracorer, and for cores 2, 3, 4 and 5 a slip hammer was used (Appendix III). Compaction of core 1 was compared with the other lake edge cores (3, 4 and 5). It was found to be considerably less ie 22% (C1) compared to 65% (C3, C4 and C5). Consequently this lower compaction explains the better definition and resolution of the sediment layering in core 1. Hence, core 1 was used to describe the stratigraphy of Old Man Lake at the lake edge.

Core 2 is used to describe the centre stratigraphy of the lake, with further knowledge of the stratigraphy being provided by a 2 m deep hole, located inland towards the east (Fig 2).

4.2.1 Stratigraphy of Core 1 (Lake Edge: North).

Core 1 is 160 cm in length (true depth ~ 2.05 cm). Fifteen distinct, fine grained sedimentary layers (C1.1 to C1.15) constitute core 1(Fig 3). A detailed description of each layer is provided in Appendix IV.

Three sedimentary sequences are proposed for core 1 (Fig 3). A partially calcretised basal-dune sequence, which consists of layer C1.15, an estuarine sequence which includes layers C1.13 through to layer C1.12. and a lacustrine sequence, comprised of the layers C1.11 through to the top layer (C1.1). Note the layer C1.14 has not been included in any of the sequences. This layer is high in organic content and is discussed in section 6.

4.2.1.1 Carbonate component grain description

The lacustrine sequence is composed of silt and clay size carbonate grains. An exception to this is observed in the top layer (C1.1), where an abundance of *Coxiella* sp. produces a coarse sand component.

Compared to the lacustrine sequence, the estuarine carbonate grains are larger in size. Carbonate grains range in size from a sand component, forming the finest fraction, through to a coarse mollusc-rich component. The upper section (C1.12) of the estuarine sequence contains a large amount of fragmented skeletal material (eg mollusc fragments) and a high proportion of sand. In contrast to this, the lower estuarine sequence is characterised by numerous articulated bi-valves and whole gastropods. The change from a non-fragmented lower estuarine sequence through to one which is highly fragmented may represent a shoaling upward sequence, and hence reflect an increase in energy levels

Carbonate grains of the basal-dune sand are similar to those in the present dune sand found surrounding Old Man Lake. This sand is composed of fragmented molluscs and other calcareous organisms.

4.2.1.2 Siliciclastic component grain description

Siliciclastics are negligible for the lacustrine sequence. The estuarine sequence contains very fine to fine, sub-rounded to sub-angular quartz sand.

The basal-dune sequence exhibits a siliciclastic texture nearly identical to the overlying estuarine sequence. Some grains show a higher degree of rounding and appear frosted.

4.2.1.3 Mineralogy

Overall mineral percentages (excluding C1.1 for lacustrine sequences) are provided below.

Lacustrine	Aragonite	18%
	Calcite	79%
	Quartz	3%
Estuarine	Aragonite	54%
	Calcite	24%
	Quartz	26%

Basal-dune Aragonite 45%
Calcite 18%
Quartz 37%

A significant increase in quartz and aragonite marks a boundary between the lacustrine and estuarine sequence. A decrease in calcite is also observed (Fig 3). An increase in aragonite is explained by the abundance of mollusc fragments dispersed throughout the estuarine sequence. Molluscs are a primary source of aragonite.

The boundary between the basal-dune sequence and the overlying estuarine sequence is not marked by such a pronounced mineral change. Instead a basal-organic unit overlies the basal-dune sequence, and separates it from the estuarine sequence.

4.2.1.4 Foraminifera

The forams *Cibicides* sp., *Elphidium advenum*, *Elphidium* (larger form), and *Quinqueloculina* sp. are observed in the estuarine sequence of Old Man Lake. *Cibicides* is common to an open marine environment, *Quinqueloculina* sp., *Elphidium* sp. can tolerate high to normal marine salinities and *Ammonia beccarii* can live in environments ranging from low to very high salinities (Li pers. comm. 1993). *Quinqueloculina* sp., *Elphidium* sp., and *Ammonia beccarii* are observed in the lacustrine sequence.

4.2.1.5 Molluscs

Lacustrine molluscs consist of: *Physastra gibbosa*, *Coxiella striata*, *Tatea rufabilabris*, *Sphaerium tasmanicum*, *Potamopyrus niger*. Estuarine sequence molluscs include *Katelysia scalarina*, *Spisula trigonella*, *Clanculus isoclanculus*, *Ostrea agassi*, *Batillari diemensis* and *Tellina albinella*. The estuarine sequence mollusc assemblage constitutes the St Kilda Formation. The St Kilda Formation may be defined as sediments deposited under marine conditions during the Holocene (Cann and Gostin 1985) and represents coastal facies associated with the Holocene sea transgression (~ 7000 radiocarbon years B.P) (Belperio and Cann 1990). *Clanculus, Katelysia and*

Batillari are marine genera, with *Coxiella* being restricted to athalassic saline water (Thoms and Williams 1993)

A good stratigraphic section of the estuarine sequence (St Kilda Formation) is observed in a hole (dimensions ~ 2m deep × 3m wide × 3m long) located north-east of core 1 (Fig 2). Beds consisting of articulated *Katelysia*, gastropods, *Ostrea* and other molluscs are seen in contact with the underlying basal-dune sequence.

4.2.1.6 Bryozoa

Bryozoa is not found in the lacustrine sequence, however species of *C. aciculata* (MacGillivray 1891, Sprigg and Bone 1993) are presently living in Old Man Lake under paralic conditions. This species was not identified in the estuarine sequence. Estuarine bryozoans include a *Cellarid*-like branching form, which is found under marine conditions, and an *Idmonea*-like family of bryozoa (probably *Nevianopora pulcherrima*). *Idmonea* is a robust, branching bryozoan and also indicates marine conditions (Bone pers. comm. 1993). A *Cellaporaria*-like bryozoan was observed encrusting an old exposed oyster (*Ostrea*) shell (St Kilda Formation), and provides another example of an estuarine bryozoa.

Echinoid plates and spines are also observed in the estuarine sequence

4.2.1.7 Hardgrounds

Hardground layers are observed to in close association with the lacustrine sequence. Thickness of the hardgrounds varied. Thin brittle types were observed alternating with thick massive hardgrounds. All hardground layers are composed of calcite (LMC). However the percentage of $MgCO_3$ appears to increase with depth (see below).

Layer	*Mineralogy*	*Depth*
C1.3 (Thin)	(2.5 mol% $MgCO_3$) Calcite	38cm
C1.5 (Massive)	(5.0 mol% $MgCO_3$) Calcite	61cm
C1.5 (Thin)	(6.5 mol% $MgCO_3$) Calcite	66cm
C1.6 (Thin)	(7.0 mol% $MgCO_3$) Calcite	86cm

As discussed in section 4, hardgrounds may form from the degassing of carbonate-rich groundwaters. Although decompression is a cause of phase saturation, so is evaporation of the aqueous phase. Evaporation removes water from equation 1, resulting in the supersaturation of the mineral phase which is then followed by precipitation. However in the lacustrine sequence of core 1 no evaporite deposits are observed. If evaporative processes were active in the past one would expect the occurrence of an evaporite deposit somewhere within the lacustrine sequence.

$MgCO_3$ contents of the lacustrine hardgrounds increase with depth. This trend may reflect the evolution of ground-water composition throughout time.

4.2.2 Stratigraphy of Core 2 (Lake Centre)

Core 2 is 128 cm in length (true depth ~370 cm) and is divided into 19 sedimentary layers (Appendix IV).

The positioning of core 2 in the lake centre results in only the sampling of the lacustrine sequence. Hence core 2 supplements the lacustrine descriptions previously discussed in 4.2.1.

4.2.2.1 Carbonate component grain description

As for core 1, the lacustrine sequence consists of very fine carbonate muds and silts. The *Coxiella* rich top layer observed for core 1 is absent from the lacustrine sequence of core 2. An explanation for this may be

due to predominating south westerly winds. When dead, *Coxiella* are swept up by wind induced currents and deposited on the north-eastern shore of the lake. Such deposits are observed today.

4.2.2.2 Other properties

Lacustrine siliciclastics are negligible for core 2. Mineral trends (Appendix V) show that with increasing depth, calcite decreases, while aragonite and quartz contents increase. *Coxiella striata*, are found dispersed throughout the lacustrine sequence.

Stromatolitic structures are observed at depth ranges of 0-3 cm, 16-21.5 cm and 126 -127 cm. Layers sampled at depth were dosed with quartz and subjected to XRD analysis (Appendix I). All consist of calcite with varying amounts of $MgCO_3$.

Sedimentary layer	***Mineralogy***
C2.1 (19.4cm)	(9.0 mol% $MgCO_3$) *major* and (2.5 mol% $MgCO_3$) *minor* calcite.
C2.5 (61.0cm)	(9.5 mol% $MgCO_3$) calcite.
C2.7 (64.0cm)	(9.0 mol% $MgCO_3$) calcite.
C2.11 (73.0cm)	(8.0 mol% $MgCO_3$) calcite.
C2.16 (98.0cm)	(12.5 mol% $MgCO_3$) *major* and (4.0 mol% $MgCO_3$) *minor* calcite.
C2.19 (128.0cm)	(13.0 mol% $MgCO_3$) *major* and (3 mol% $MgCO_3$) *minor* calcite.

Hardground layers, which occurred frequently throughout the lacustrine sequence of core 1, are absent in the lacustrine sequence of core 2. However the trend of increasing $MgCO_3$ content within calcites is still observed. One explanation may be due to the overburden of water (~3m deep) inhibiting degassing of any ground-water, and therefore retarding

cementation. Minerals are formed but not to the degree required for extensive hardground formation.

The stratigraphy of Old Man Lake records the sedimentary events from approximately 7000 years BP up until present time. The estuarine sequence represents a major early to mid Holocene marine lagoon complex, which existed between the Woakwine and Robe Ranges. The lagoon/estuarine complex formed as a result of a Holocene marine transgression which reached present sea level approximately 7000 years BP (Belperio and Cann 1990).

The estuarine sequence of Old Man Lake compares favourably to the Holocene bioclastic sediments found at an excavation site of Fresh Dip Lake which lies 800m north-east. Amino acid racemisation age determinations gave a mid-Holocene age to estuarine *Katalysia* valves (Belperio and Cann 1990). The estuarine sequence of Fresh Dip Lake indicates shoaling upwards. Subtidal oyster and echinoids are observed at the base of the sequence. Intertidal sediments containing articulated *Katalysia* and *Anapella* overlie the basal section. Finally the stratigraphy of the upper portions of the sequence are highly fragmented and represent intertidal sand flat sedimentation (Belperio and Cann 1990).

The lacustrine stratigraphy of Old Man Lake represents a relative fall of sea level associated with tectonic uplift and hydro-isostatic warping of the region. The uplift produced a 0.5 to 1m fall in Holocene sea level (Belperio and Cann 1990). At some stage in its geological history Old Man Lake became seperated from Lake Eliza which lies to the east.

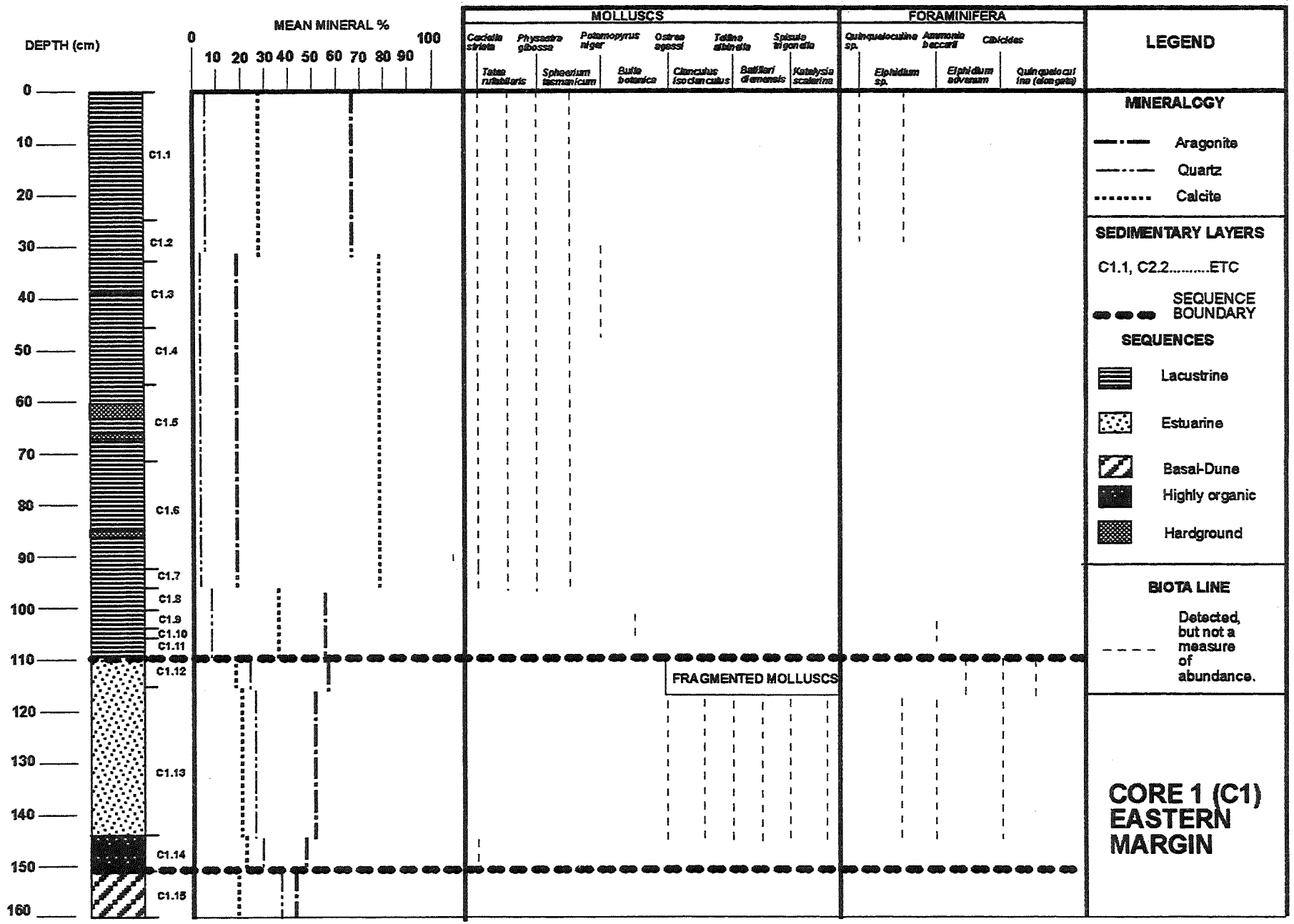

Fig 3. Mineralogy and biota associatons of core 1

5. Organic Analysis of Old Man Lake Cores

Five samples, C1M, C2M, C3M, C4M and C5M were taken from a middle organic unit (MOU) of each core. The MOU corresponds to the muddy chocolate-brown layer of the lacustrine sequence, C1.5 (47.0-71.8 cm) . C4TT-BB and C5TT-BB were sampled from a basal organic unit (BOU), with BB and TT representing the lower and upper basal organic units, respectively. The basal organic unit is equivalent to the layer C1.14 (144.0-151.0 cm) of core 1, a black organic-rich layer bounded below by a basal dune sequence and above by an estuarine sequence.

Representing the lower MOU is the sample, C5B. For the purpose of Rock-eval interpretation, both C5M and C5B are considered as the one sample, C5MB. Grouping of these two samples is based upon the similarity of their geochemical parameters. For gas chromatography analysis each sample is assessed independently, hence both upper and lower MOU are discussed.

Rock-eval pyrolysis and gas chromatography were performed on each of the above samples (Appendix I).

5.1 Rock-eval pyrolysis

Total organic carbon (TOC) values from MOU samples range from 6.04 wt.% (C1M) to a maximum of 19.56 (C2M) wt.% with an average of 10.3 wt.%. BOU values range from 1.47 (C4BB) to 29.12% (C4TT), with an average of 11.6 wt.%. Lower BOUs for cores 4 and 5 had considerably less TOC values compared to the upper BOU values. Lower BOUs have less TOC values (average 1.52 wt.%) compared upper BOUs (average 21.7 wt.%).

Hydrogen indices from both the middle and basal units are highly variable. For the MOUs a maximum HI of 595.0 mg HC/g TOC is recorded for sample C2M. The lowest HI occurs for sample C3M, which has a value of 278.0 mg HC/g TOC. The basal organic unit HIs vary from 465.0 mg HC/g TOC (C4BB) to 108.0 mg HC/g TOC (C5BB). The average hydrogen index for the middle organic unit (432

mg HC/g TOC) is significantly higher than the basal organic unit average (240 mg HC/g TOC).

T(max) values for all MOU samples exhibit little deviation. The Average T(max) for the MOUs is 429°C. For the BOUs the average T(max) is considerably lower (403°C) and again, as for TOC values, significant differences in T(max) are observed for the upper and lower basal organic units. Average T(max) for the lower and upper BOUs is 422°C and 384°C respectively. The T(max) for all organic samples is less than 435°C, indicating immature organic matter (Peters and Moldowan 1993).

Sample	T(max)°C	S1	S2	S3	S1+S2	PI	S2/S3	TOC	HI	OI
C1M	429.00	13.97	23.98	100.38	37.95	0.37	0.24	6.04	397.00	1662.0
C2M	426.00	50.59	116.42	56.14	167.01	0.30	2.07	19.56	595.00	287.0
C3M	435.00	12.22	26.50	42.98	38.72	0.32	0.62	9.53	278.00	451.0
C4M	429.00	17.69	35.42	14.97	53.11	0.33	2.37	6.37	556.00	235.0
C5MB	428.00	21.18	33.45	22.12	54.63	0.39	1.51	10.01	334.00	221.0
C4TT	388.00	27.96	61.13	175.30	89.09	0.31	0.35	29.12	210.00	602.0
C4BB	426.00	0.30	6.83	2.78	7.13	0.04	2.46	1.47	465.00	189.0
C5TT	380.00	12.85	25.64	38.43	38.49	0.33	0.67	14.34	179.00	268.0
C5BB	418.00	0.83	1.69	2.81	2.52	0.33	0.60	1.57	108.00	179.0

Table 2. Rock-eval pyrolysis results

S1: Thermally distilled hydrocarbons (mg HC/g rock).

S2: Hydrocarbons generated by pyrolytic degradation of the kerogen in the rock (mg HC/g rock).

S3: Milligrams of carbon dioxide generated from a gram of rock during temperature programming up to 390°C.

T.O.C: Total Organic Carbon (wt.%).

T(max): Temperature at which the maximum amount of S2 HCs are generated (° C).

HI: Quantity of pyrolyzable organic compounds relative to T.O.C (mg HC/g T.O.C).

OI: Quantity of carbon dioxide from S3 relative to T.O.C (mg CO_2/g T.O.C).

PI: Production index {S1/(S1 +S2)}

(Peters and Moldowan 1993)

Assuming a vitrinite reflectance of 0.6%, TOC values indicate that both the upper basal and middle organic units have a very good hydrocarbon generative potential, according to Peters and Moldowan (1993) (ie a TOC greater than 2 wt.%). The lower BOU is considered to be a good generator. Other generative geochemical parameters, S1, S2 and S1+S2, are not satisfied and hence the assignment of a generation potential is only tentative. Likewise, caution must be taken in the allocation of kerogen types. T(max), being an integral part of the above kerogen classification scheme, is a crude measurement of thermal maturity and is, in part, controlled by the type of organic matter (Peters and Moldowan 1993). Many of the geochemical parameters determined by rock-eval pyrolysis assume a VR of 0.6%. This again warrants caution.

A Van Krevelen diagram of HI vs T(max) plots most organic samples within the realm of a Type III kerogen (Appendix VI). C5BB is placed in kerogen type IV, wheras C2M plots as a Type II kerogen. The samples, C1M, C2M, C3M, C4M and C4BB, are scattered along the line of 0.5% VR (vitrinite reflectance). C5TT and C5BB have much lower reflectances. Therefore, the middle organic unit is assumed to be a Type II-III kerogen, whereas the basal organic unit represents a Type III-IV kerogen.

Hayball *et al.* (1993) used a HI vs T(max) Van Krevelen diagram in describing the organic facies of North Stromatolite Lake, Coorong South Australia. Kerogen precursor types were described as:

Type I-II: Comprising of *Botryococcus braunii* (abundant). Filamentous cyanobacteria (common to abundant). No recognisable plant remains . Dominated by n-heptadecane and n-$C_{21}$to C_{33} homologues, with a marked odd/even predominance (OEP at n-C_{27} =2.4-4.3). Trace of the acyclic isoprenoids.

Type II Filamentous algae are abundant. *B. braunii* is rare. Terrestrial plant detritus (cutinite, inertinite) is common. Pristane and 2,6,10-

	trimethyl-7-(3-methylbutyl)-dodecane are dominant aliphatic hydrocarbons. The latter may be derived from the green algae *Enteromorpha* sp. (Rowland *et al.* 1985).
Type II-III/III	Define an inverse relationship between HI and TOC contents. Such a relationship may reflect varying degrees of oxygenation at the sediment-water interface. The variation may be caused by differences in bioturbation. Coccoid cyanobacteria and higher plants (including the grass-like metaphyte, *Ruppia* sp.) are major kerogen precursors.
Type IV	Inertinite material.
	(Hayball *et al.* 1993)

Hence such precursor materials and associated trends, may also hold true for the kerogen types of Old Man Lake.

5.2 Gas Chromatography

SAMPLE	OEP	CPI	C-25 HBI/n-C31
C1M	10.58	9.47	0.77
C2M	3.86	5.65	0.57
C3M	10.84	7.64	5.91
C4M	5.95	8.61	0.27
C5M	6.03	8.71	0.24
C5B	6.61	7.43	0.69
C4TT	*	*	*
C4BB	1.27	8.50	0.00
C5TT	23..60	19.42	0.01
C5BB	5.43	5.83	0.00

*** No results available**

Table 3. Gas Chromatographic Geochemical Parameters.

$$CPI = \left[\frac{C_{25}+C_{27}+C_{29}+C_{31}+C_{33}}{C_{26}+C_{28}+C_{30}+C_{32}+C_{34}} + \frac{C_{25}+C_{27}+C_{29}+C_{31}+C_{33}}{C_{26}+C_{28}+C_{30}+C_{32}+C_{34}} \right] \div 2$$

$$OEP = \frac{C_{21}+6C_{23}+C_{25}}{4C_{26}+4_{28}}$$

CPI = Carbon Preference Index

OEP = Odd -Even Predominance

Pr/Ph = Pristane / Phytane Ratio

(Peters and Moldowan 1993)

5.2.1 Middle Organic Unit

The middle organic unit is characterised by the appearance of the acyclic C_{25}- highly branched isoprenoids (n-C_{25}-HBI) which elutes between the normal alkanes of C_{21} and C_{22} (Appendix II). This highly branched alkane is considered be a derivative of the acyclic C_{25} alkadiene, a marine diatomaceous biomarker. In Hamelin Pool, Shark Bay Western Australia, the C_{25} alkadiene was most prominent in diatom-dominated microbial mats. These mats represent laminated microbialites and are involved in the construction of subtidal stromatolites (Summons *et al.* 1993). Stromatolites are layered microbialites. As well as diatoms, algae may present another possible source for the highly branched isoprenoid (Rowland and Robson 1990). The highly branched isoprenoids are seen to decrease in number when going from the lower MOU (C5B: C-25 HBI/ n-C31=0.69) to the upper MOU (C5M: C-25 HBI/ n-C31=0.24) (Table 3). A transition from restricted saline, to a less saline conditions may explain such a change in C_{25} HBI concentrations.

The MOU n-alkanes exhibit a large odd predominance between C_{22} and C_{33} (eg OEP (C3M)= 10.84) with a peak at n-C_{31}. The chromatogram is skewed towards the n-C_{22} to n-C_{31} range. Many unidentifiable compound (⊕ Appendix II) are observed eluting between C_{34}-C_{35} (C4M) and C_{18}-C_{19}. The large odd predominance over this carbon range may possibly indicate a non marine algae input (Peters and Moldowan 1993), though such highly branched alkanes generally imply a higher plant source. A terrestrial plant source is also supported by a peak at n-C_{31}.

5.2.2 Basal Organic Unit

C_{25} highly branched isoprenoids are absent in the lower basal organic unit, while only a trace is detected for the upper BOU. The lower BOU has a bi-modal distribution of normal alkanes with peaks at both n-C_{16} and n-C_{31}. An odd predominance is present, though not to the same extent as that of MOU.

The upper BOU is skewed towards the carbon range C_{22}-C_{33} and peaks at n-C_{25}. The organic unit has a large odd predominance (OEP (C5TT) = 23.6)

The difference in alkane distribution observed between the upper and lower BOUs may be explained by a change in organic source. The higher branched alkanes indicate higher terrestrial plant matter. A peak shift is interpreted as a change from terrestrial conditions, dominated by higher plants, to an environment with an increasing algal/bacterial input. HBIs detected in traceable amounts may possibly support this interpretation. Diatoms may have bloomed when conditions were favourable.

6. Discussion

The Holocene history of Old Man Lake can be postulated according to organic, stratigraphic and lateral facies variations.

Stage 1 Pre-Holocene Transgression

Old Man Lake occupies a vegetated back dune hollow, to the west lies the Southern Ocean and to the east an interdunal corridor which is connected to Old Man Lake by a topographical low. The sea is at low stand and calcrete formation is active, and results in the formation of the partially calcretised basal-dune sequence.

Stage 2 Activation of the Holocene Transgression

Beginning of the Holocene sea transgression. A rise in sea level produces a rise in ground-water level. The water table rises and outcrops in the Old Man Lake region producing marsh-like conditions. At first the emerging ground-water reflects the composition of the freshwater lens that is kept buoyant by the invading saline marine wedge. With time the ground-water outcrops become increasingly more saline, resulting in the destruction of certain land plants and the propagation of new saline-tolerant organisms. The marsh conditions provide a poor environment of organic preservation and results in a Type III-IV kerogen. The lower BOU provides evidence of higher terrestrial plant material. The upper BOU, with the appearance of C-25 highly branched isoprenoids, indicates the onset of restricted saline conditions.

Stage 3 Marine Incursion

At some stage prior to the mid-Holocene, sea water breached the Robe Range and flooded the Robe-Woakwine interdunal corridor. The flooding produced a lagoonal depositional environment. Old Man Lake, connected to the corridor via a topographical low flanking its south-eastern margin, experienced the marine inundation. The marine inundation is represented by the estuarine sequence.

Stage 4 Thrombolite formation

Thrombolite formation is observed in contact with subtidal oyster beds of the estuarine sequence. The association of thrombolites with zones of

ground-water discharge may indicate an increase in subsurface inflow. Increasing subsurface inflow may reflect a period of higher rainfall and hence indicate a humid climate. Wet conditions prevailed in south-eastern South Australia between 6900 and 5000 years BP and again marginally between 2000 and 1300 BP (Dodson 1974). Evidence of an increased freshwater input is indicated by the occurrence of bryozoa *C. aciculata* and the green luminescence characteristic of freshwater aragonite. The formation of thrombolite would have then diminished following the onset of relatively more dry conditions.

Stage 5 Marine Regression

Tectonic uplift and hydro-isostatic warping of south-eastern South Australia resulted in a relative fall in Holocene sea level. The shoaling estuarine sequence provides evidence of this marine regression.

Stage 6 Lake Partitioning

Old Man Lake was isolated from the main lagoon during a fall in Holocene sea level. The estuarine sequence of Old Man Lake already exhibits shoaling. Winds moving sand northwards would have produced a barrier across the topographical low, resulting in the segregation of Old Man Lake from the main lagoon. Partitioning resulted in lacustrine sedimentation resulting in the deposition of the lacustrine sequence. C-25 HBI appear at the base of the lacustrine sequence and diminish with decreasing depth. The isoprenoid trend reflects the withdrawal of a marine wedge associated with the fall in Holocene sea level. Lacustrine calcitic hardgrounds also mirror the fall in sea level as the hardground become progressively deficient in $MgCO_3$. Marine waters are high in Mg concentration. A Type II-III kerogen represented in the lacustrine sequence may indicate the contribution of higher plant terrestrial matter. The colonisation of dunes by land plant material would be expected as the sea level fell.

7. Conclusion

i) Old Man Lake contains three major sequences. A partially calcretised basal-dune sequence which is in turn overlain by an estuarine sequence. Overlying the estuarine sequence is the lacustrine sequence. Each sequence reflects different sedimentary environments which were primarily controlled by sea level fluctuations. Kerogen type distribution and the appearance of highly branched isoprenoids (C25-HBI) provides additional information on Holocene sedimentation.

Organic and sequence analyses shows the transition of Old Man Lake throughout the Holocene :

a) An interdunal hollow stabilised by vegetation and under the influence of calcretisation processes

b) A marine incursion and subsequent ground-water rise and deposition of Type III-IV kerogen followed by biocalstic estuarine deposits.

c) A fall in sea level and onset of lacustrine sedimentation.

ii) The distribution of thrombolite indicates an increase in ground-water input, which is attributed to a wetter climate in the past. The associations of *C.aciculata* with thrombolite and the green luminescence of aragonitic gastropods within the thrombolite further support this freshwater influence.

iii) The study of green luminescing aragonite requires further investigation. Being associated with freshwater and reflecting an increase in Mn concentration, CL studies of lacustrine carbonates within coastal areas, or areas with considerable aragonite input, may provide an insight into flow regimes of palaeoaquifers. This information could be then utilised in trying to determine ground-water response to climatic change.

8. References

Barsanov, G.P. & Sarsembaeva, K.K. Luminescence of Iceland spar: *Tr. Mineralog. Muzeya Akad. Nauk,* v. 13, 147.

Bayly, I.A.E. (1970) Further studies on some saline lakes of south-east Australia: *Australian Journal of Marine and Freshwater Research,* v. 21, 117-129.

____& Williams, W.D. (1966) Chemical and Biological Studies on some saline lakes of south-east Australia: *Australian Journal of Marine and Freshwater Research,* v.17, 177-228.

Belperio, A.P. & Cann, J.H. (1990) Quaternary evolution of the Robe-Naracoorte coastal plain: an excursion guide: *Dept. Mines and energy, report book No. 90/27.*

Bone, Y. (1991) Population explosion of the bryozoan *Membranipora aciculata* in the Coorong Lagoon in late 1989: *Aust. J. Earth Science,* v. 38, 121-123.

____& Wass, R. (1990) Sub-Recent bryozoan- serpulid buildups in the Coorong Lagoon, South Australia: *Ibid.* v. 37, 207-216.

Burne, R.V. & Ferguson, J. (1983) Contrasting marginal sediments of a seasonally flooded saline lake - Lake Eliza, South Australia: significance for oil shale genesis: *BMR Journal of Australian Geology and Geophysics,* v.8, 99-108.

____& Moore, L.S. (1987) Microbialites: Organosedimentary deposits of benthic microbial communities: *Palaios* v. 2, 241-254.

Cann, J.H. & Gostin, V.A. (1985) Coastal sedimentary facies and foraminiferal biofacies of the St Kilda Formation at Port Gawler, South Australia: *Trans. R. Soc. S.Aust.,* v. 109(4), 121-142.

Dodson, J.R. (1974) Vegetation history and water fluctuations at Lake Leake, south-eastern South Australia. I. 10,000 B.P. to Present: *Aust. J. Bot.,* v. 22, 719-41.

Hayball, A.J. (1990) Organic geochemistry of Holocene lacustrine carbonates in the Coorong region, South Australia: BSc.(Hons) thesis, The Flinders University of South Australia.

____ McKirdy, D.M., Warren, J.K., von der Borch, C.C. & Padley, D. (1991) Organic facies of Holocene carbonates in North Stromatolite Lake, Coorong region, South Australia: *15th International Meeting on Organic Geochemistry, Manchester, U.K., Programme and Abstracts,* 19-20.

Holmes, J.W. & Waterhouse, J.D (1983) *Hydrology*: In; Natural History of the South East. Tyler, M.J., Twidale, C.R., Ling, J.K., and Holmes, J.W. South Australia.

Hossfield, P.S. (1950) The Late Cainozoic history of the south-east of South Australia: *Trans. R. Soc. S.Aust.,* v. 73, 232-279.

James, N.P. & Choquette, P.W. (1990) *The meteoric diagenetic environment*: In; Diagenesis. McLLreath, I.A & Morrow, D.W., 35-75. Geoscience Canada.

Kennard, J.M. & James, N.P. (1986) Thrombolites and stromatolites: Two distinct types of Microbial structure: *Palaios,* v. 1, 492-503.

Kröger, F.A. (1948) Some aspects of the luminescence 1,2 of solids. Elsevier, Amsterdam, 310 p.

Last, W.L. (1992) Petrology of modern carbonate hardgrounds from East Basin Lake, a saline marr lake, southern Australia: *Sedimentary Geology,* v. 81, 215-229.

Linwood, S.H. & Weyl, W.A. (1942) The fluorescence of manganese in glasses and crystals: *J. Opt. Soc. Am,* v. 32, 443-445.

MacGillivray, P. H. (1891) Description of new or little known polyzoa: *Trans. R. Soc. S.Aust.,* v. 3, 77-83.

McCunn, H.J. (1972) Calcite and aragonite phenomena precipitated by organic decay in high lime concentrate brines: *J. Sedim. Petrol.,* v. 42 (1), 150-154.

Moore, L.S. (1987) Water chemistry of the coastal saline lakes of the Clifton-Preston lakeland system, south-western Australia, and its influence on stromatolite formation: *Aust. J. Marine & Freshwater Res.*, v. 38, 647-660.

____Knott, B. & Stanley, N. (1984) The stromatolites of Lake Clifton: Living structures represent the origins of life: *Search* v. 14, 309-314.

Nelson, R.G. (1972) Electrical resistivity investigations in the south-east of South Australia: *South Aust. Dept. Mines. Quarterly Geological Notes,* No. 42, 7-10.

Osiko, V.V. & Maksimova, G.V. (1960) Valence of the manganese activator in crystal phosphors: *Opt. Spectr. (USSR) Engl. Transl.* v. 9, 248.

Peters, K.E. & Moldowan, J.M. (1993) The biomarker guide: Interpreting fossils in petroleum and ancient sediments. Prentice Hall.

Rowe, K. (1992) Depositional history, facies and mono-hydrocalcite of a small, permanent lake near Robe, south-eastern South Australia: BSc.(Hons) thesis, The University of Adelaide, South Australia.

Rowland, S.J., Yon, D.A., Lewis, C.A., & Maxwell, J.R. (1985) Occurrence of 2,6,10-trimethyl-7-(3-methylbutyl) dodecane and related hydrocarbons in the green alga *Enteromorpha prolifera* and sediments: *Org. Geochem* v. 8, 207-213.

Rowland, S.J. & Robson, J.N. (1990) The widespread occurrence of highly branched acyclic C_{20}, C_{25} and C_{30} hydrocarbons in Recent sediments and biota- A review: *Marine Environmental Research,* v. 30, 191-216.

Schwebel, D.A. (1983) *Quaternary dune systems*: In; Natural History of the South East. Tyler, M.J., Twidale, C.R., Ling, J.K., and Holmes, J.W. South Australia.

Sommer, S. E. (1972) Cathodoluminescence of carbonates:
1. Characterisation of cathodoluminescence from carbonate solid solutions, 257-273.
2. Geological applications, 275-284
Chemical Geology, v. 9, 257-284.

Sprigg, M. & Bone, Y. (1993) Bryozoa in Coorong-type lagoons, southern Australia: *Trans. R. Soc. S.Aust.*, v. 117(2), 87-95.

Sprigg, R.C. (1952) Geology of the south-east province of South Australia, with special reference to Quaternary coastline migrations and modern beach developments: *Geology. Surv. S. Aust. Bull.*, v. 29.

Summons, R.E., Barrow, R.A., Capon, R.J., Hope., J.M. & Stranger, C. (1993) The structure of a new C_{25} isoprenoid alkene biomarker from diatomaceous microbial communities: *Aust. J. Chem.*, v. 46, 907-915.

Taylor, G.F. (1975) The occurrence of monohydrocalcite in two small lakes in the south-east of South Australia: *Am. Miner.*, v. 60, 690-697.

Thoms, M.C. & Williams, W.D, (1993) The sediments of Lake Cantara South, a saline lake in South Australia: *Int. J. Salt Lake Res.*, v. 2(1), 29-40.

von der Borch, C.C. (1976) Stratigraphy and formation of Holocene dolomitic carbonate deposits of the Coorong area, South Australia: *J. Sedim. Petrol.*, v. 46, 952-966.

____Lock, D.E. & Schwebel, D.A. (1975) Groundwater formation of dolomite in the Coorong region of South Australia: *Geology,* v. 3, 283-285.

____Balda, J.L. & Schwebel, D.A. (1980) Amino acid racemisation dating of the Late Quaternary strandline events of the coastal plain near Robe, south-eastern South Australia: *Trans. R. Soc .S. Aust.*, v 104(6), 167-170.

Warren, J.K. (1982) The hydrological setting, occurrence and significance of gypsum in late Quaternary salt lakes in South Australia: *Sedimentology,* v. 29, 609-637.

___ **(1988)** Sedimentology and mineralogy of dolomitic Coorong Lakes, South Australia: *J. Sedim. Petrol.,* v. 60(6), 843-858.

Wright, V.P. (1992) A revised classification of limestones: *Sedimentary Geology,* v. 76, 177-185.

APPENDIX I

Analytical Techniques

ANALYTICAL TECHNIQUES

A. TOC analysis

Total organic carbon analysis of the organic material was performed at The Flinders University Of South Australia.

B. Solvent Extraction

Solvent extraction was done according to Hayball (1990).

Analytical reagent grade solvents were distilled through a 60 cm fractionating column prior to their use in the extraction process.

Soxhlet extraction was used to remove any extractable organic matter (EOM) in the samples. This was accomplished by placing a pre-weighed amount of each crushed sample into a pre-extracted thimble, plugged with cotton wool. The thimble was located within the Soxhlet apparatus and extracted for about 24 hours with an azeotropic mixture consisting of 186 ml of dichloromethane (DCM) and 14 ml of methanol. Prior to extraction, activated copper turnings were added to the solvent to remove any elemental sulphur incorporated within the sediment.

Excess solvent was removed using a rotary evaporator and the concentrated EOM transferred to a pre-weighed vial. Residual solvent in the vial was evaporated with a heating block and the total EOM reported in ppm and mg/g TOC. The EOM was redissolved in the DCM and stored under refridgeration.

C. Column and Gas Chromatography

Column and gas chromatography was done according to Hayball (1990)

Column Chromatography

A 40 cm glass column was plugged with cotton wool, filled with petroleum ether and packed with a slurry of activated silica and petroleum ether. Approximately 1g of activated silica was then

added to to the top of the packed column. The EOM was transferred dropwise to about 2 g of activated alumina and the excess solvent driven off by stirring with a spatula before being carefully transferred to the top of the prepared column.

Separation of the EOM into aliphatic, aromatic and polar compounds was carried out by eluting with 120 ml of the following solvent mixtures:

Aliphatics - petroleum ether 100%
Aromatics - petroleum ether : dichloromethane (40:60)
Polars - dichloromethane : methanol (35:65)

Excess solvent from each fraction of the EOM was removed with a rotary evaoproator and the residue transferred to pre-weighed vials from which the mass of each fraction could be calculated after final evaporation of the remaining solvent.

Gas Chromatography (GC)

The total saturated hydrocarbon (*viz n*-alkanes, branched and cyclic alkanes) fraction and the naphthene (*viz* branched and cyclic alkanes) fraction were examined by gas chromatography using the following instrumental parameters:

Instrument	Varian 3400
Injector	On-column
Column	30 mm x 0.25 mm fused silica, DB-1
Carrier Gas	Hydrogen with a linear flow rate of 30 $cmsec^{-1}$
Temperature programming	60° for 2 minutes, ramped at 4°C per minute to 300°C and held isothermal at 300°C for 20 minutes
FID temperature	305°C

D X-ray Diffraction (XRD) Analysis

Ten drops of deionised water were added to two heaped microspatular amounts of sample and then ground by mortar and pestle to form the required slurry.

The slurry was then smeared over 2/3 of a clean and labelled slide. After drying the sample was then subjected to XRD analysis under the following conditions:

Defractometer	Philips PW105
Monochromator	Graphite
Radiation Source	Cobalt Kα radiation. Wavelength 1.7902 Å
2-θ Scanning Range	3° to 75° with a step interval of 0.05°

JCPDS Manuals were used in the identification of minerals.

A modification of the below equation was used to determine mineral percentages.

$$\% \text{ Aragonite} = \frac{5P(A).100}{5P(A)+P(C)+P(Q)}$$

$$\% \text{ Calcite} = \frac{P(C)}{5P(A)+P(C)+P(Q)}$$

$$\% \text{ Quartz} = \frac{P(Q)}{5P(A)+P(C)+P(Q)}$$

(Adapted from von der Borch 1976)

Where P(A), P(C) and P(Q) are equal to the peak heights of aragonite, calcite and quartz respectively. $MgCO_3$ mol% were determined by dosing the samples with quartz.

E. Cathodoluminescence (CL) Analysis

Instrument	Technosyn Cold Stage Luminoscope
Film	Ektachrome PC1600
Average Operating Conditions	16 kV and gun current 240 μa
Sample	Polished Thin Sections

F. Rock-eval

Rock-eval was performed at AMDEL, Thebarton, S.A.

APPENDIX II

Gas Chromatography Results

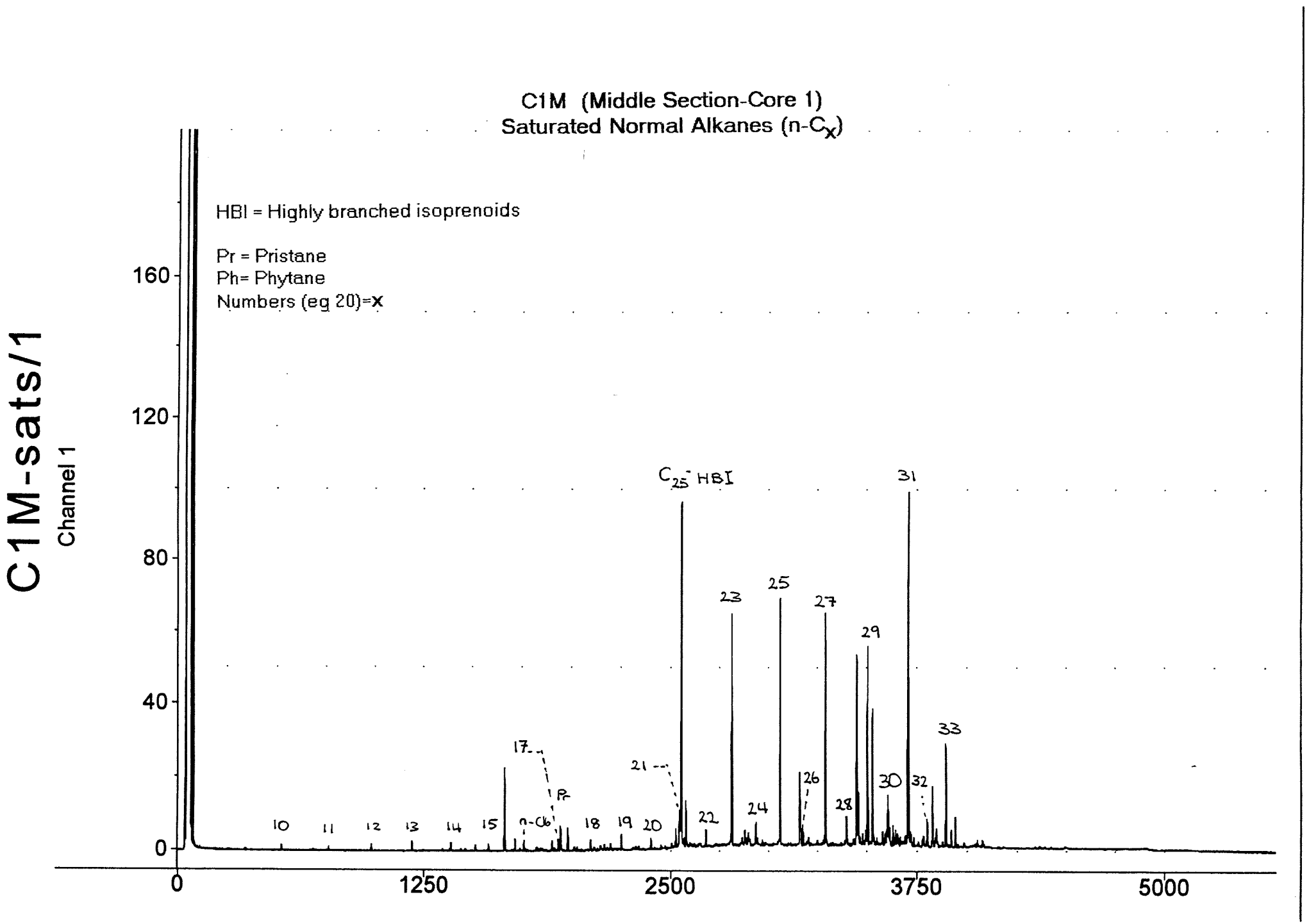
C1M (Middle Section-Core 1)
Saturated Normal Alkanes (n-Cx)
HBI = Highly branched isoprenoids
Pr = Pristane
Ph= Phytane
Numbers (eg 20)=x
C1M-sats/1
Channel 1
160
120
80
40
0
0
1250
2500
3750
5000
C25 HBI
31
23
25
27
29
33
17
Pr
21
26
30
32
28
24
22
10
11
12
13
14
15
n-C16
18
19
20

C2M (Middle Section-Core 2)
Saturated Normal Alkanes (n-C_X)

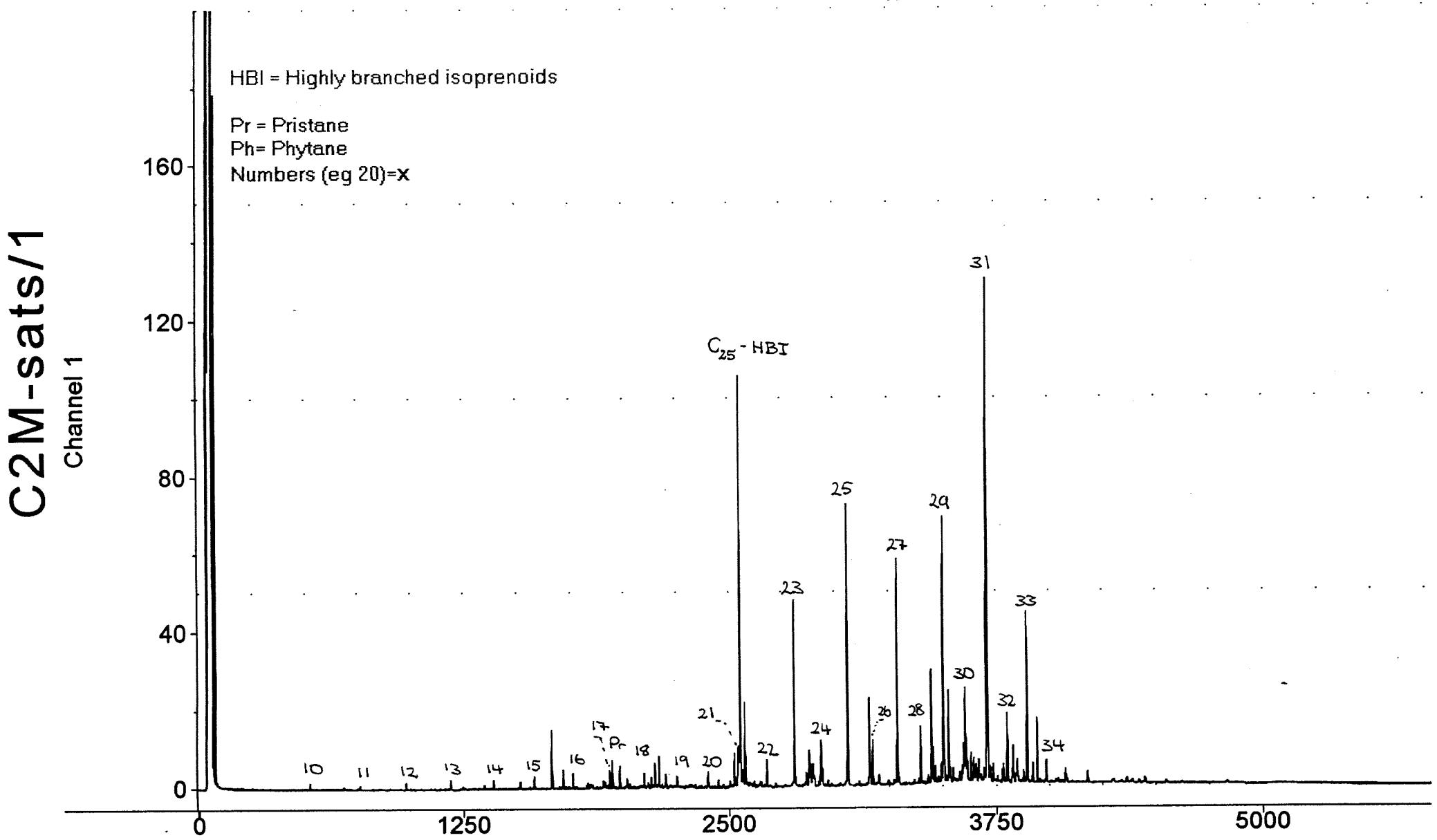

C3M (Middle Section-Core 3)
Saturated Normal Alkanes (n-C_x)

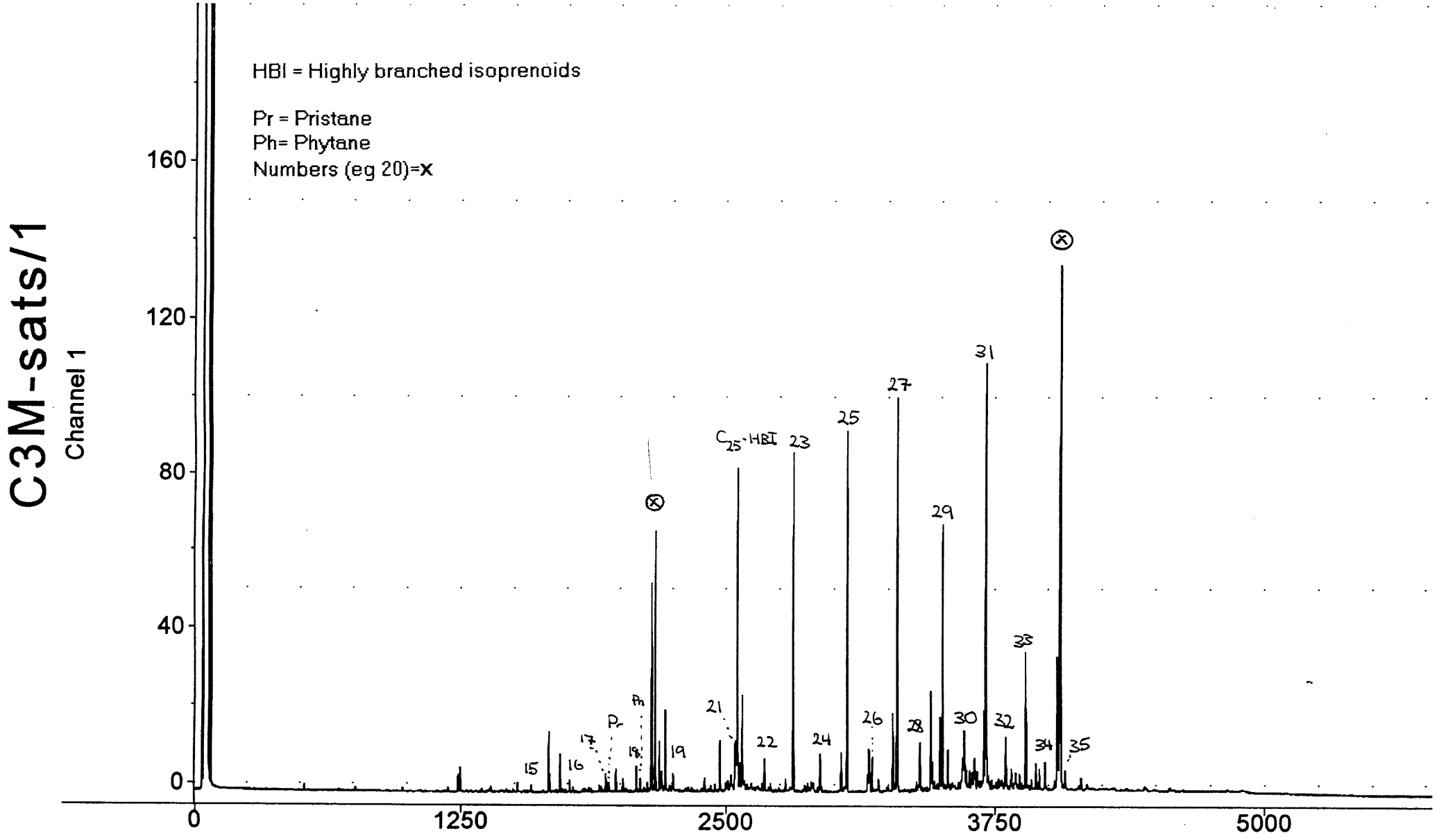

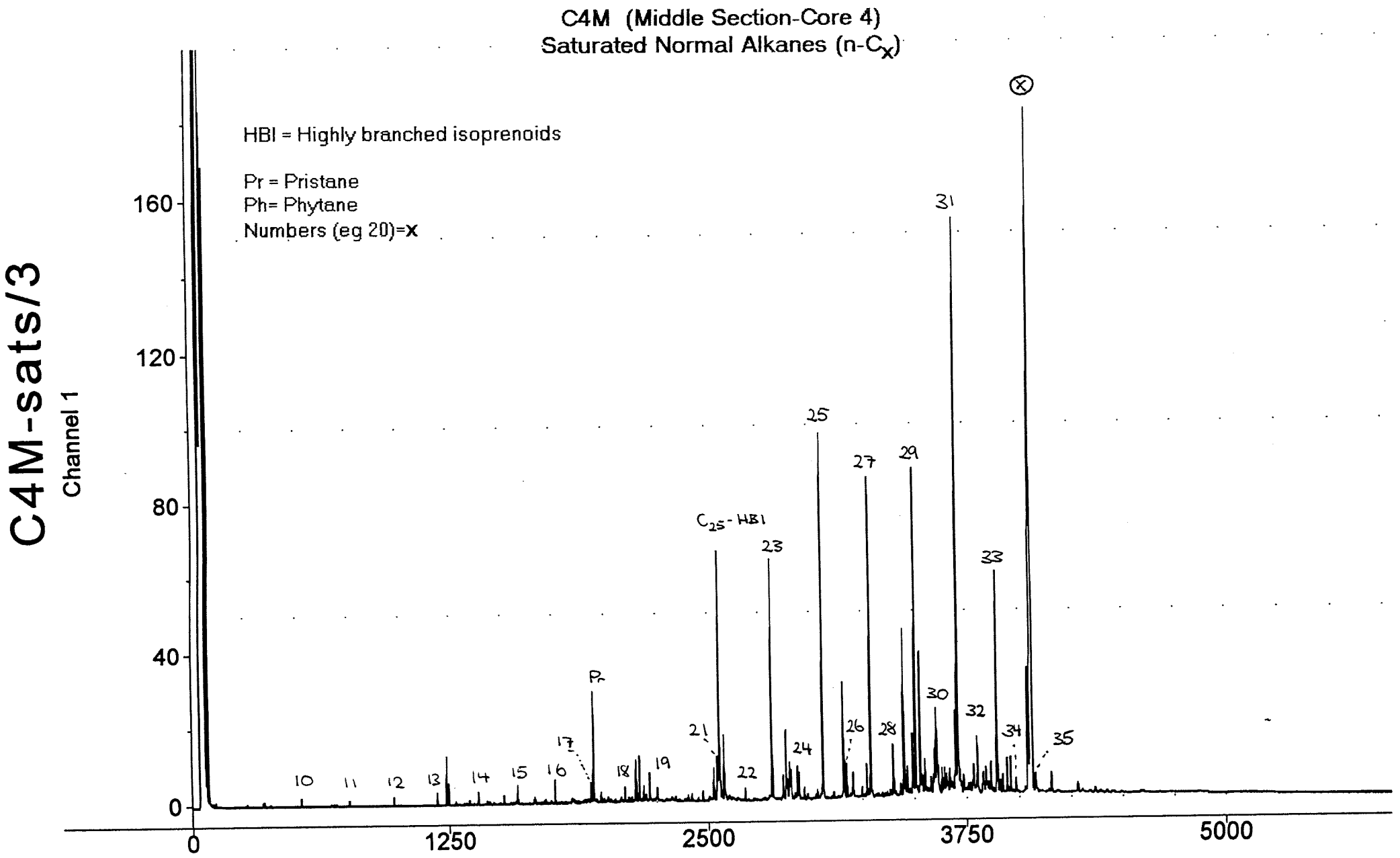
C4M (Middle Section-Core 4)
Saturated Normal Alkanes (n-Cx)
HBI = Highly branched isoprenoids
Pr = Pristane
Ph= Phytane
Numbers (eg 20)=x
C4M-sats/3
Channel 1
160
120
80
40
0
0
1250
2500
3750
5000
10
11
12
13
14
15
16
17
Pr
18
19
21
C25- HBI
22
23
24
25
26
27
28
29
30
31
32
33
34
35

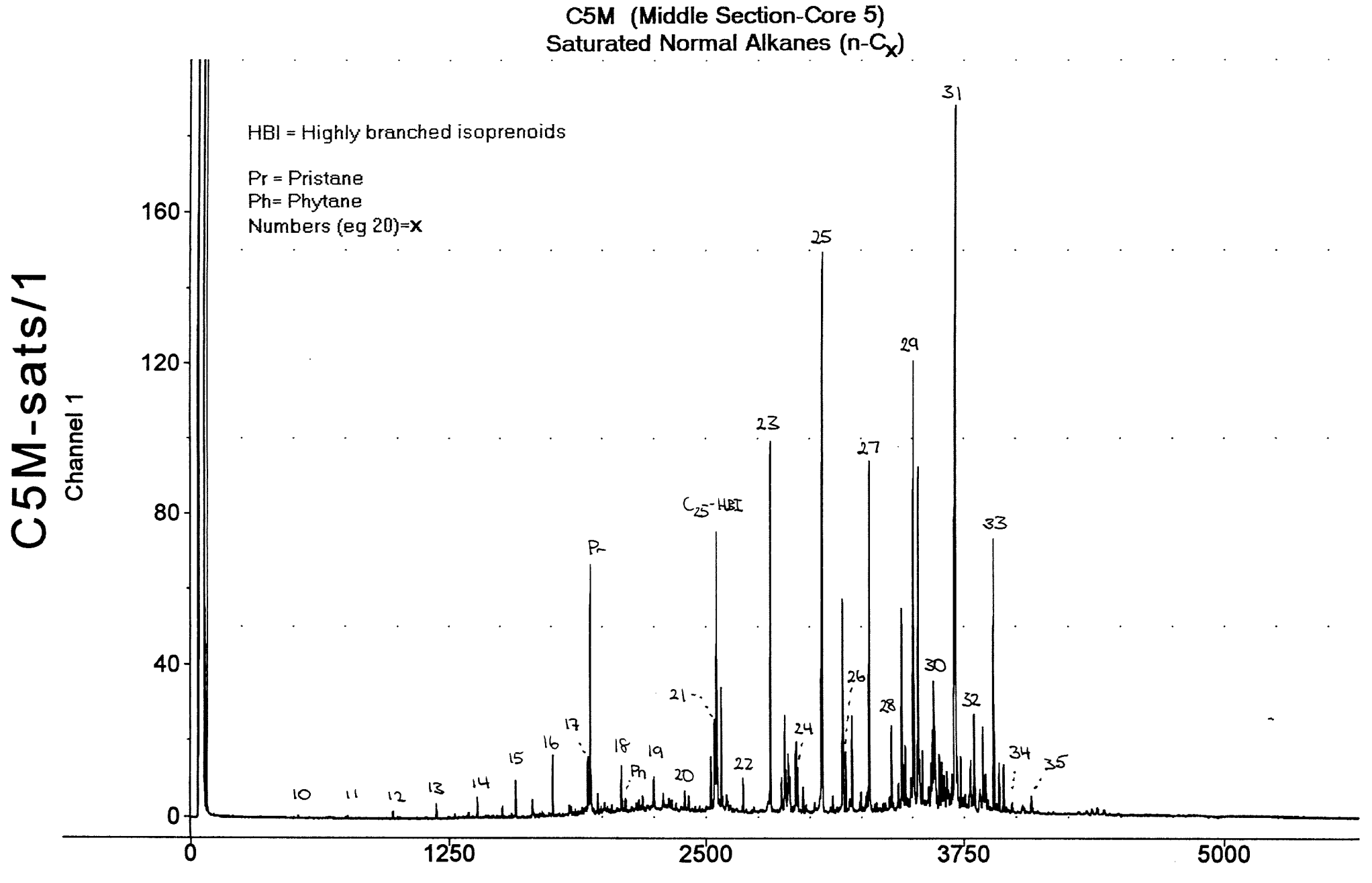
C5M (Middle Section-Core 5)
Saturated Normal Alkanes (n-Cx)
HBI = Highly branched isoprenoids
Pr = Pristane
Ph= Phytane
Numbers (eg 20)=x
C5M-sats/1
Channel 1
0
40
80
120
160
0
1250
2500
3750
5000
10
11
12
13
14
15
16
17
Pr
18
Ph
19
20
21
C25-HBI
22
23
24
25
26
27
28
29
30
31
32
33
34
35

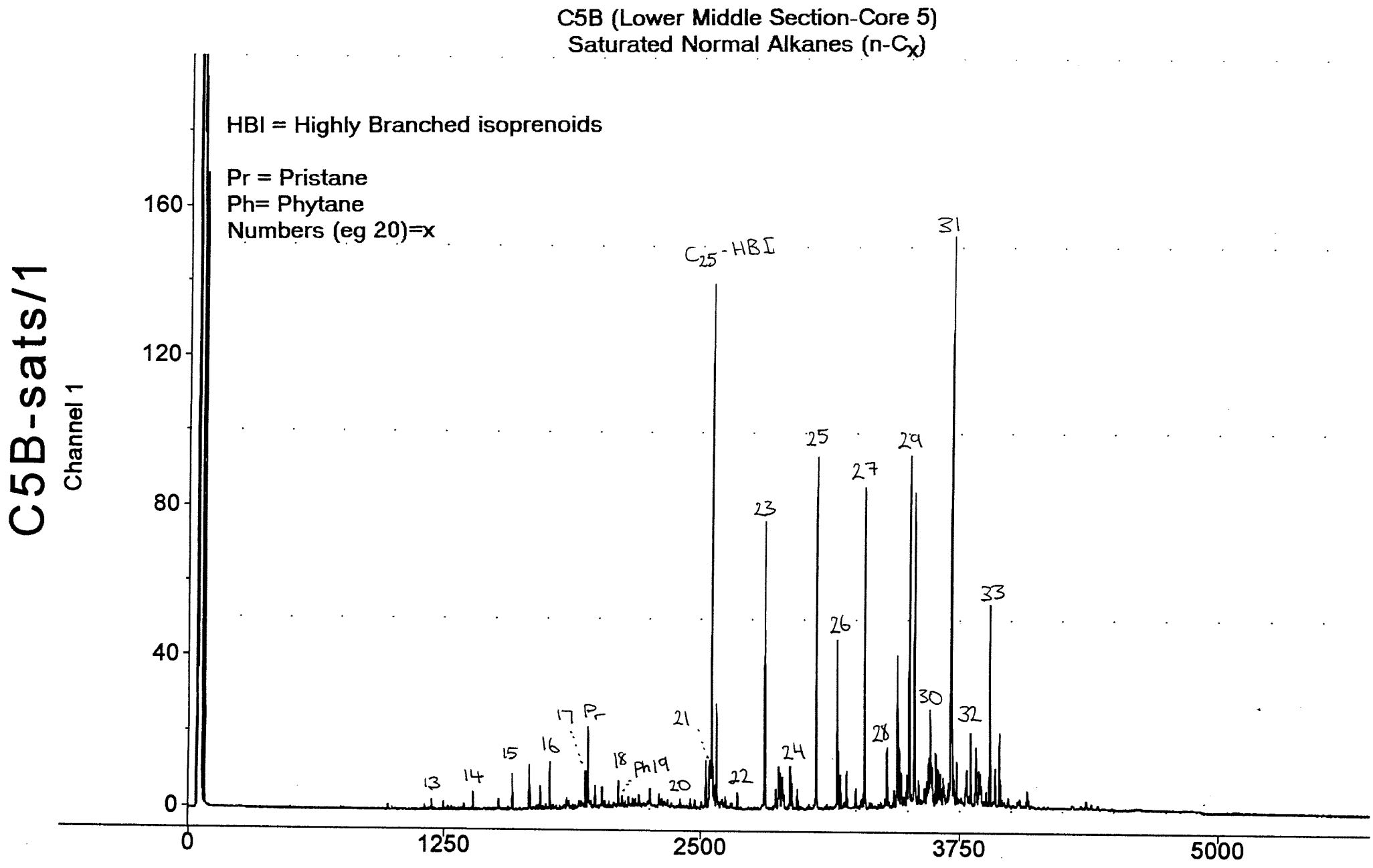
C5B (Lower Middle Section-Core 5)
Saturated Normal Alkanes (n-Cx)
HBI = Highly Branched isoprenoids
Pr = Pristane
Ph= Phytane
Numbers (eg 20)=x
C5B-sats/1
Channel 1
160
120
80
40
0
0
1250
2500
3750
5000
C25-HBI
31
25
29
27
23
26
33
30
32
28
24
22
21
17 Pr
18
Ph19
20
16
15
14
13

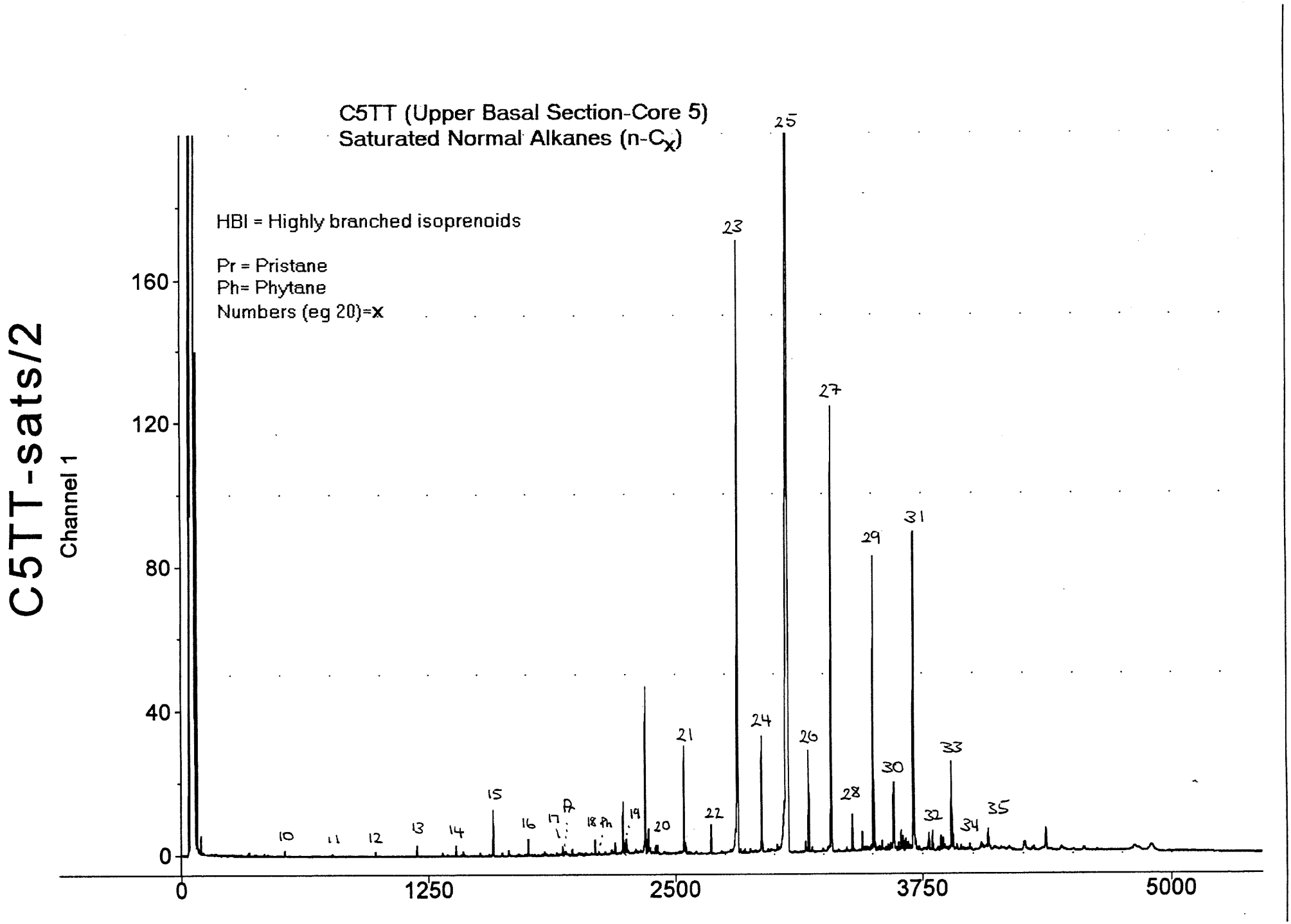
C5TT (Upper Basal Section-Core 5)
Saturated Normal Alkanes (n-Cx)
HBI = Highly branched isoprenoids
Pr = Pristane
Ph= Phytane
Numbers (eg 20)=x
C5TT-sats/2
Channel 1
160
120
80
40
0
0
1250
2500
3750
5000
10
11
12
13
14
15
16
17
Pr
18
Ph
19
20
21
22
23
24
25
26
27
28
29
30
31
32
33
34
35

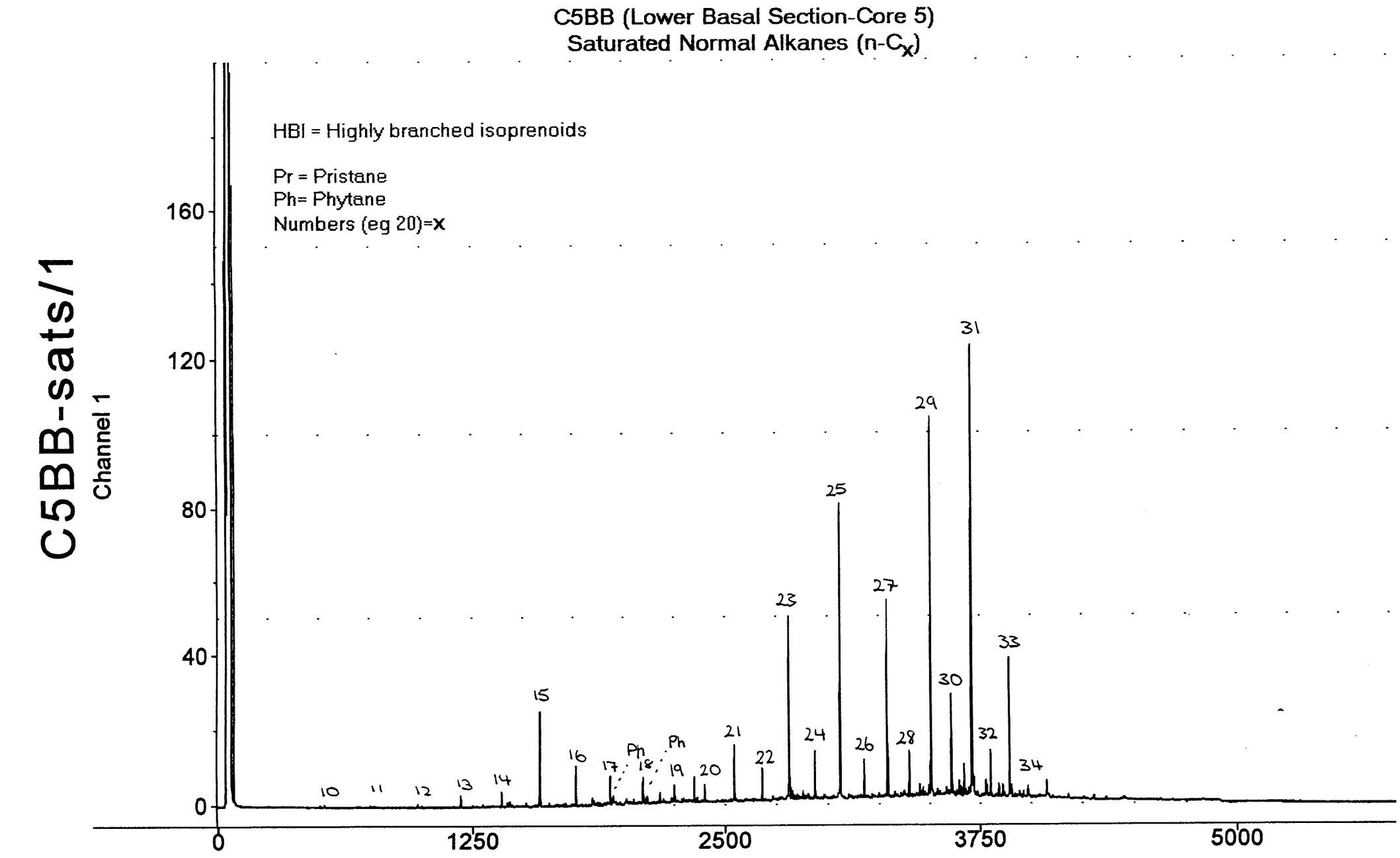
C5BB (Lower Basal Section-Core 5)
Saturated Normal Alkanes (n-Cx)
HBI = Highly branched isoprenoids
Pr = Pristane
Ph= Phytane
Numbers (eg 20)=x
C5BB-sats/1
Channel 1
160
120
80
40
0
0
1250
2500
3750
5000
10
11
12
13
14
15
16
17
Pr
18
Ph
19
20
21
22
23
24
25
26
27
28
29
30
31
32
33
34

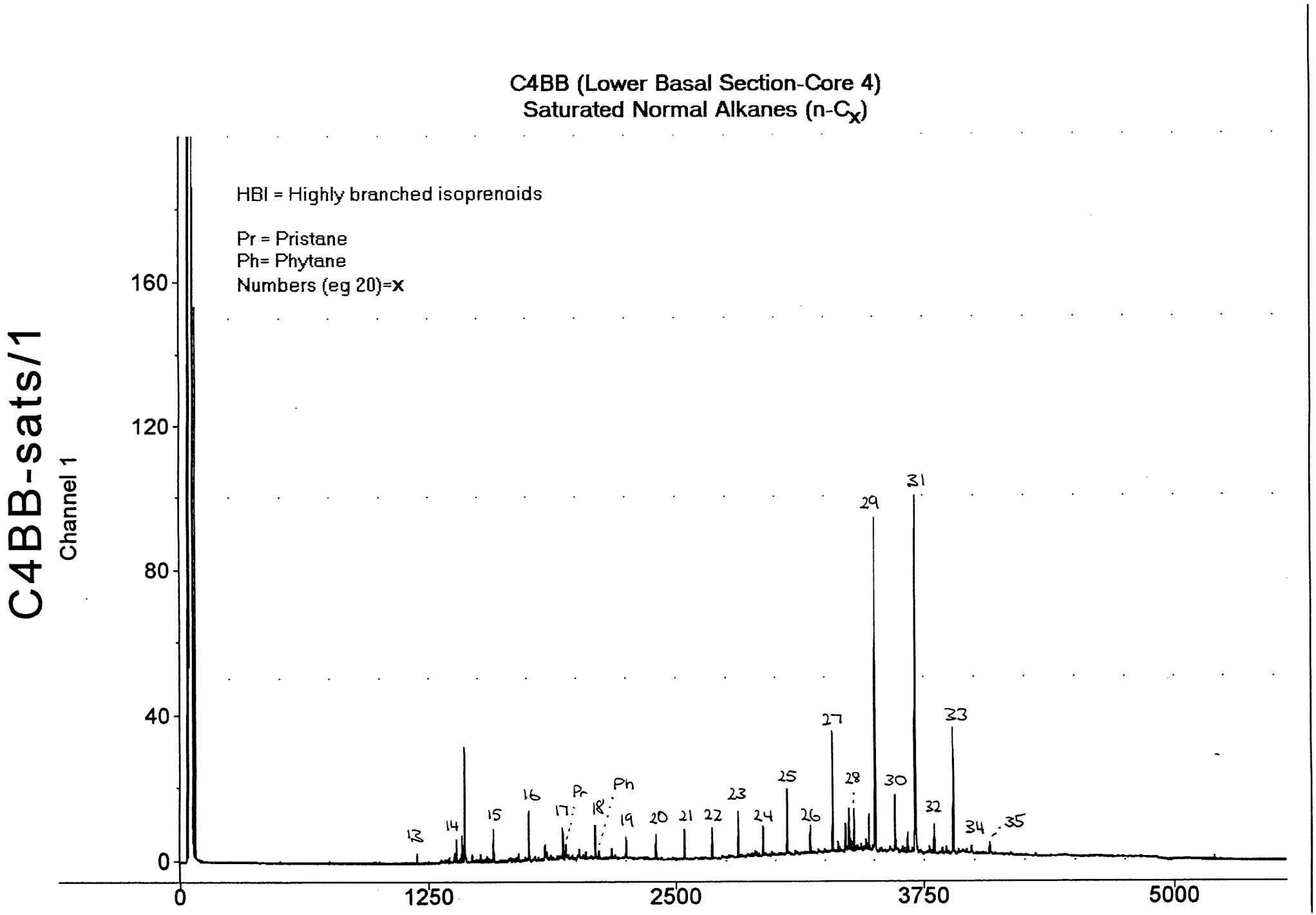
C4BB (Lower Basal Section-Core 4)
Saturated Normal Alkanes (n-Cx)
HBI = Highly branched isoprenoids
Pr = Pristane
Ph= Phytane
Numbers (eg 20)=x
C4BB-sats/1
Channel 1
160
120
80
40
0
0
1250
2500
3750
5000
13
14
15
16
17
Pr
18
Ph
19
20
21
22
23
24
25
26
27
28
29
30
31
32
33
34
35

Gas Chromatography Information

C1M-SATS/1

Organic Compound	Retention Time (sec)	Area (mV.s)	Height (mv)
n-C16	1763.25	6.26	2.34
n-C17	0.00	0.00	0.00
Pristane	1946.25	20.62	6.00
n-C18	0.00	0.00	0.00
Phytane	0.00	~0	~0
n-C19	2253.50	9.20	3.29
n-C20	0.00	0.00	0.00
n-C21	2546.00	51.23	9.49
C25-HBI	2556.25	357.60	94.83
n-C22	2680.75	11.83	0.00
n-C23	2814.75	238.29	63.04
n-C24	2938.00	24.16	5.61
n-C25	3062.50	232.40	67.20
n-C26	3176.75	14.39	4.90
n-C27	3293.25	238.58	62.95
n-C28	3400.00	26.10	7.11
n-C29	3507.50	193.32	53.30
n-C30	3607.50	57.14	12.45
n-C31	3711.50	463.09	96.53
n-C32	3802.75	20.48	6.18
n-C33	3896.50	94.82	27.08
n-C34	0.00	0.00	0.00

C.P.I	9.47
O.E.P	10.58
Pr/Ph	>>>1
C25HBI/C31	0.77

C2M-SATS/1

Organic Compound	Retention Time (sec)	Area (mV.s)	Height (mv)
n-C16	1762.25	10.93	3.69
n-C17	1933.50	10.80	3.92
Pristane	1945.25	25.48	6.61
n-C18	2096.75	8.38	3.15
Phytane	0.00	~0	~0
n-C19	2253.00	8.62	2.18
n-C20	0.00	0.00	0.00
n-C21	2544.50	61.25	9.50
C25-HBI	2555.25	391.45	104.30
n-C22	2680.00	16.60	5.90
n-C23	2812.50	162.12	46.50
n-C24	2937.00	52.60	10.61
n-C25	3061.50	270.45	71.03
n-C26	3175.75	32.67	10.80
n-C27	3291.25	212.35	57.40
n-C28	3398.50	51.74	14.27
n-C29	3507.25	270.42	67.37
n-C30	3607.00	106.70	23.42
n-C31	3711.50	692.77	127.97
n-C32	3801.75	59.23	16.92
n-C33	3896.25	150.11	42.66
n-C34	3985.00	14.67	4.83

C.P.I	5.65
O.E.P	3.86
Pr/Ph	>>>1
C25HBI/C31	0.57

Gas Chromatography Information

C3M-SATS/1

Organic Compound	Retention Time (sec)	Area (mV.s)	Height (mv)
n-C16	1761.75	5.80	2.31
n-C17	1933.25	10.90	4.02
Pristane	0.00	0.00	0.00
n-C18	2096.25	7.60	2.73
Phytane	0.00	0.00	0.00
n-C19	2252.25	16.20	3.98
n-C20	0.00	0.00	0.00
n-C21	2544.25	76.50	11.89
C25-HBI	2554.00	294.30	82.47
n-C22	2679.75	21.40	7.01
n-C23	2813.75	332.80	86.63
n-C24	2936.50	20.30	7.30
n-C25	3062.00	358.20	90.96
n-C26	3175.50	18.10	6.64
n-C27	3292.75	411.50	99.78
n-C28	3398.25	38.00	10.89
n-C29	3506.75	254.40	66.48
n-C30	3606.25	50.20	12.19
n-C31	3698.75	49.80	16.51
n-C32	3801.25	33.60	10.77
n-C33	3895.75	135.70	33.21
n-C34	3984.75	16.50	5.50

C.P.I	7.64
O.E.P	10.84
Pr/Ph	0.00
C25HBI/C31	5.91

C4M-SATS/3

Organic Compound	Retention Time (sec)	Area (mV.s)	Height (mv)
n-C16	1762.50	15.90	5.55
n-C17	1934.00	12.70	4.61
Pristane	1946.25	100.30	28.79
n-C18	2097.25	8.30	3.19
Phytane	0.00	~0	~0
n-C19	2253.25	9.60	2.72
n-C20	0.00	0.00	0.00
n-C21	2544.00	61.40	10.73
C25-HBI	2554.50	235.70	65.49
n-C22	2680.00	5.40	21.90
n-C23	2813.75	221.00	62.95
n-C24	2937.00	21.70	7.80
n-C25	3063.25	401.80	95.79
n-C26	3176.25	20.00	7.34
n-C27	3293.25	333.90	83.88
n-C28	3399.75	55.20	12.70
n-C29	3509.50	400.00	86.16
n-C30	3607.75	113.70	21.58
n-C31	3713.75	857.40	151.08
n-C32	3802.50	55.80	13.94
n-C33	3898.00	241.30	57.90
n-C34	3985.50	8.40	2.83

C.P.I	8.61
O.E.P (1)	5.95
Pr/Ph	>>>1
C25HBI/C31	0.27

Gas Chromatography Information

C5M-SATS/1

Organic Compound	Retention Time (sec)	Area (mV.s)	Height (mv)
n- C16	n.p	n.p	n.p
n-C17	1931.75	44.50	13.79
Pristane	1944.50	243.10	64.45
n-C18	2094.75	32.10	10.90
Phytane	2113.75	9.70	2.34
n-C19	2250.50	30.40	7.67
n-C20	0.00	0.00	0.00
n-C21	2541.00	113.60	22.88
C25-HBI	2552.00	288.80	72.46
n-C22	2677.50	16.10	6.73
n-C23	2812.75	376.50	95.55
n-C24	2934.50	51.20	17.40
n-C25	3062.75	807.20	147.30
n-C26	3174.00	40.60	13.69
n-C27	3291.00	387.40	90.72
n-C28	3397.50	91.20	20.67
n-C29	3508.25	580.10	117.51
n-C30	3605.50	133.00	31.78
n-C31	3712.50	1218.90	183.86
n-C32	3800.00	86.50	22.22
n-C33	3895.75	272.50	68.82
n-C34	0.00	0.00	0.00

C.P.I	8.71
O.E.P	6.03
Pr/Ph	25.1
C25HBI/C31	0.24

C5TT-SATS/2

Organic Compound	Retention Time (sec)	Area (mV.s)	Height (mv)
n-C16	n.p	n.p	n.p
n-C17	1933.50	3.70	1.70
Pristane	0.00	0.00	0.00
n-C18	2096.75	9.40	3.40
Phytane	0.00	0.00	0.00
n-C19	2253.75	16.90	3.40
n-C20	0.00	0.00	0.00
n-C21	2544.25	97.20	29.10
C25-HBI	2552.00	5.10	2.20
n-C22	2679.75	20.30	7.10
n-C23*	2818.25	946.20	169.60
n-C24	2938.25	0.00	29.34
n-C25*	3074.50	2494.30	199.18
n-C26	3177.00	66.20	23.84
n-C27	3294.75	560.30	119.98
n-C28	3398.50	21.40	7.45
n-C29	3507.75	320.10	79.84
n-C30	3609.50	100.30	17.26
n-C31	3709.50	390.20	86.73
n-C32	3801.00	10.10	3.88
n-C33	3895.50	80.10	23.49
n-C34	0.00	0.00	0.00

C.P.I	19.42
O.E.P	23.60
Pr/Ph	0.00
C25HBI/C31	0.01

Gas Chromatography Information

C5BB-SATS/1

Organic Compound	Retention Time (sec)	Area (mV.s)	Height (mv)
n-C16	1763.50	23.60	10.48
n-C17	1934.50	19.40	6.81
Pristane	1950.00	5.87	1.53
n-C18	2097.75	16.30	5.78
Phytane	0.00	~0	~0
n-C19	2253.50	7.60	2.90
n-C20	0.00	0.00	0.00
n-C21	2544.75	39.00	13.45
C25-HBI	0.00	0.00	0.00
n-C22	2681.00	20.30	7.22
n-C23	2813.50	161.10	47.58
n-C24	2938.25	32.70	11.13
n-C25	3062.75	289.70	77.60
n-C26	3177.00	24.10	8.42
n-C27	3292.00	180.40	51.04
n-C28	3399.50	35.50	10.86
n-C29	3509.75	459.50	100.78
n-C30	3608.00	79.60	25.80
n-C31	3719.00	5.80	2.31
n-C32	3802.50	26.40	9.59
n-C33	3897.00	116.30	34.19
n-C34	0.00	0.00	0.00

C.P.I	5.83
O.E.P	5.43
Pr/Ph	>>>1
C25HBI/C31	0.00

C4BB-SATS/1

Organic Compound	Retention Time (sec)	Area (mV.s)	Height (mv)
n-C16	1762.75	37.90	12.64
n-C17	1933.50	23.40	7.80
Pristane	1949.75	16.90	3.49
n-C18	2097.00	27.50	8.40
Phytane	2116.25	6.13	1.51
n-C19	2252.25	16.10	5.30
n-C20	0.00	0.00	0.00
n-C21	2543.50	21.80	7.40
C25-HBI	0.00	0.00	0.00
n-C22	2679.75	24.40	7.89
n-C23	2811.25	37.20	12.07
n-C24	2937.00	24.20	7.57
n-C25	3059.00	58.70	17.38
n-C26	3175.75	21.00	6.91
n-C27	3290.50	108.70	32.54
n-C28	3398.75	38.90	10.77
n-C29	3508.50	392.60	91.02
n-C30	3606.50	47.30	14.68
n-C31	3710.25	440.40	97.21
n-C32	3801.50	11.00	6.77
n-C33	3896.00	97.60	33.43
n-C34	0.00	0.00	0.00

C.P.I	8.50
O.E.P	1.27
Pr/Ph	2.76
C25HBI/C31	0.00

Gas Chromatography Information

C5B-SATS/1

Organic Compound	Retention Time (sec)	Area (mV.s)	Height (mv)
n-C16	1763.25	37.30	12.04
n-C17	1934.50	27.90	9.07
Pristane	1946.50	88.60	20.63
n-C18	2097.75	17.10	6.03
Phytane	2116.00	6.20	1.77
n-C19	2253.50	9.60	3.15
n-C20	0.00	0.00	0.00
n-C21	2545.00	76.30	11.52
C25-HBI	2557.25	610.20	138.45
n-C22	2680.75	7.80	3.05
n-C23	2814.75	274.00	75.10
n-C24	2937.50	21.90	8.19
n-C25	3063.00	372.10	92.37
n-C26	3176.50	20.80	7.50
n-C27	3293.50	320.20	83.49
n-C28	3400.50	58.30	14.60
n-C29	3510.00	384.40	91.67
n-C30	3608.50	129.10	23.54
n-C31	3714.25	887.70	149.89
n-C32	3803.25	71.00	17.80
n-C33	3898.00	199.60	51.89
n-C34	3986.00	2.90	1.22

C.P.I	7.43
O.E.P	6.61
Pr/Ph	14.3
C25HBI/C31	0.69

APPENDIX III

Coring Methods

CORING METHODS

Two coring methods were utilised in obtaining cores from Old Man Lake.

Core 1 was obtained using a Wacka Vibracorer (8 cm diameter). For cores 2, 3, 4 and 5 a slip hammer was used (5 cm diameter).

The slip hammer was quicker and easier to use, however the compaction levels were significantly higher when compared to the cumbersome vibracorer. These factors need to be taken into consideration when selecting a coring method.

APPENDIX IV

Detailed Core Descriptions

DETAILED CORE DESCRIPTIONS

CORE 1

LAYER C1.1 (Top Layer)

Depth: **0.0 - 25.5cm**

Colour: Light creamy brown

Carbonate Grains And Other Components: The Coarse fraction (>2mm) is dominated by gastropods (ranging up to 4mm in length), ostracods and small bivalves. Calcareous fragments constitute the finer mud matrix.

Siliciclastic Grains: Negligible.

Mineralogy: 68% Aragonite, 27% calcite and 5% quartz. The major source of aragonite is supplied by the unaltered gastropods.

Foraminifera: *Quinqueloculina* sp. and *Elphidium* sp.

Mollusc Types: *Physastra gibbosa*, *Coxiella striata*, *Tatea rufabilabris* and possibly *Sphaerium (Musculium) tasmanicum*.

Organic Analysis: Not performed.

XRD Carbonate Analysis: Not performed

LAYER C1.2

Depth: **25.5 - 33.0cm**

Colour: Creamy brown.

Carbonate Grains And Other Components: Carbonate grains are the same as that of C1.1, except there are fewer gastropods.

Siliciclastic Grains: Negligible.

Mineralogy: As for Layer C1.1.

Foraminifera: As for Layer C1.1.

Mollusc Types: Fewer molluscs compared to Layer C1.1. *Physastra gibbosa*, *Coxiella striata* and *Tatea rufabilabris*

Organic Analysis: Not performed.

XRD Carbonate Analysis: Aragonite mineralogy is given for molluscs sampled at 19cm. For the fine mud fraction, at 31cm, XRD gives a (10 mol% $MgCO_3$) asymmetrical calcite peak, indicating two compositions of high Mg-Calcite (HMC).

LAYER C1.3

Depth: **33.0 - 47.0cm**

Colour: Chocolate brown.

Carbonate Grains And Other Components: Calcareous mud matrix with brittle, platey hardground material. The coarse mollusc component is the same as Layer 2, but not as abundant. Hardground material is associated with organic rich sediment.

Siliciclastic Grains: Negligible.

Mineralogy: 18% Aragonite , 79% calcite and 3% quartz.

Foraminifera: Not sampled.

Mollusc Types: Rare *Tatea rufabilabris* and possibly *Potamopyrus niger.*

Organic Analysis: Sampled from 33.0 to 40.0 cm (C1T).

C.P.I	-	T_{max}	438°C	S1+S2	22.53
O.E.P (1)	-	T.O.C	3.21	P.I	0.36
Pr/Ph	-	H.I	449		
C25HBI/C31	-	O.I	129		

XRD Carbonate Analysis: A sample of hardground material from 38.0cm revealed a mineralogy of (2.5 mol% $MgCO_3$) calcite (LMC).

LAYER C1.4

Depth: **47.0 - 57.0cm**

Colour: Orange-brown

Carbonate Grains And Other Components: Death assemblage of gastropods found from 47.0 to 47.2cm. From 47.2 to 51.2cm, abundant ostracods associated with calcareous silt. At 51.2cm observe massive blocky hardground calcareous material (0.5cm thick). Below hardground up to 57.0cm continuation of calcareous silt. Some coarse size molluscs still present.

Siliciclastic Grains: Negligible.

Mineralogy: As for Layer C1.3.

Foraminifera: Not sampled.

Mollusc Types: As for Layer C1.3.

Organic Analysis: Not performed.

XRD Carbonate Analysis: Coxiella band from 47.0cm has a mineralogy dominated by aragonite with traces of (3 mol% $MgCO_3$) calcite (LMC).

LAYER C1.5

Depth: **47.0 - 71.8cm**

Colour: Black grading into chocolate brown, with increasing depth.

Carbonate Grains And Other Components: Calcareous silt from 57.0 to 60.0cm. From 60.0 to 71.0cm re-appearance of hardground material (Both

massive and platey types). Ostracod death assemblage between 71.0 and 71.8cm. Molluscs dispersed throughout Layer in small quantities.

Siliciclastic Grains: Negligible.

Mineralogy: As for Layer C1.3.

Foraminifera: Not sampled.

Mollusc Types: As for Layer C1.3.

Organic Analysis: Sampled from 60.0 to 66.0cm (C1M).

C.P.I	9.47	T_{max}	429°C	S1+S2	37.95
O.E.P (1)	10.58	T.O.C	6.04	P.I	0.37
Pr/Ph	>>>1	H.I	397		
C25HBI/C31	0.77	O.I	1162		

XRD Carbonate Analysis: Massive hardground sampled at 61.0cm has a (5 mol% $MgCO_3$) calcite (IMC) mineralogy. Platey friable hardground sampled at 66.0cm has a (6.5 mol% $MgCO_3$) calcite (IMC) composition.

LAYER C1.6

Depth: **71.8 - 93.0cm**

Colour: Black grading into chocolate brown, with increasing depth.

Carbonate Grains And Other Components: Ostracod death assemblage from 71.0 to 78.1cm, associated with organic rich material. Friable fibrous hardground between 78.0 and 87.0cm. Where as between 87.0 and 93.0cm hardground is more sheet-like in appearance. Molluscs still present in minimal amounts.

Siliciclastic Grains: Negligible.

Mineralogy: As for Layer C1.3.

Foraminifera: Not sampled.

Mollusc Types: As for Layer C1.3.

Organic Analysis: Done from 88.0 to 93.0 cm (C1B).

C.P.I	-	T_{max}	430°C	S1+S2	67.23
O.E.P (1)	-	T.O.C	7.6	P.I	0.41
Pr/Ph	-	H.I	536		
C25HBI/C31	-	O.I	187		

XRD Carbonate Analysis: Ostracod carapaces from 74.0 cm depth have a mineralogy of (2 mol% $MgCO_3$)calcite (LMC). Platey hardground (86cm) material has a (7 mol% $MgCO_3$) calcite mineralogy.

LAYER C1.7

Depth: **93.0 - 96.5cm**
Colour: Creamy brown.
Carbonate Grains And Other Components: Calcareous silt, with molluscs being very rare.
Siliciclastic Grains: Negligible.
Mineralogy: As for Layer C1.3.
Foraminifera: Not sampled.
Mollusc Types: Rare.
Organic Analysis: Not performed.
XRD Carbonate Analysis: Not performed.

LAYER C1.8
Depth: **96.5 - 101.0cm**
Colour: Light cream grading into a cream-brown with increasing depth.
Carbonate Grains And Other Components: Calcareous mud with no molluscs.
Siliciclastic Grains: Negligible.
Mineralogy: 56% Aragonite, 36% calcite and 8% quartz.
Foraminifera: Not sampled.
Mollusc Types: Not present.
Organic Analysis: Not performed.
XRD Carbonate Analysis: A light cream Layer from 98.0cm revealed a (9 mol% $MgCO_3$) calcite (HMC) composition.

LAYER C1.9
Depth: **101.0 - 104.5cm**
Colour: The Layer grades in colour from an orange-brown at the top, through to light brown in the middle and finally dark brown at the bottom.
Carbonate Grains And Other Components: Grains vary from top to bottom. Calcareous orange-brown silt. Organic rich, mud-like sediments constitute the darker portions of the Layer. A black organic rich band is found from 103.5 to 104.5cm.
Siliciclastic Grains: Negligible.
Mineralogy: As for Layer C1.8
Foraminifera: Not sampled.
Mollusc Types: The gastropod *Bulla botanica* is the only mollusc represented in the Layer.
Organic Analysis: Not performed.
XRD Carbonate Analysis: Not performed.

LAYER C1.10

Depth: **104.5 - 106.5cm**

Colour: Cream-brown

Carbonate Grains And Other Components: Calcareous silt with a coarser fraction consisting of small gastropods.

Siliciclastic Grains: Negligible.

Mineralogy: As for Layer C1.8

Foraminifera: A trochospiral form (unidentifiable) and *Ammonia beccarii*.

Mollusc Types: *Bulla botanica* is the only mollusc represented in the Layer.

Organic Analysis: Not performed.

XRD Carbonate Analysis: Not performed.

LAYER C1.11

Depth: **106.5 - 109.0cm**

Colour: Khaki green-brown

Carbonate Grains And Other Components: Calcareous silt with no molluscs.

Siliciclastic Grains: Negligible.

Mineralogy: As for Layer C1.8

Foraminifera: Not sampled.

Mollusc Types: Not present or rare.

Organic Analysis: Not performed.

XRD Carbonate Analysis: Not performed.

LAYER C1.12

Depth: **109.0 - 116.0cm**

Colour: Khaki green.

Carbonate Grains And Other Components: Calcareous sand grains, together with aragonitic mollusc fragments make up most of the Layer. At approximately 114.0cm whole gastropods appear. At the base of the Layer, fragments of echinoid and bivalves are observed.

Siliciclastic Grains: Sub-rounded to sub-angular well sorted quartz sand.

Mineralogy: 57% Aragonite, 19% calcite and 24% quartz.

Foraminifera: *Elphidium advenum, Quinqueloculina* (c.f *elongata*) and *Cibicides* (Open Marine).

Mollusc Types: Fragmented and hence hard to identify. Most probably reworked C1.13.

Organic Analysis: Not performed.

XRD Carbonate Analysis: Not performed.

LAYER C1.13

Depth: **116.0 - 144.0cm**

Colour: Mottled grey.

Carbonate Grains And Other Components: Calcareous grains range from coarse to sand size. Both whole and fragmented molluscs are observed. Branching bryozoa, bivalves, gastropods, echinoids (plates and spines) and oyster valves are observed. Some bivalves are articulated.

Siliciclastic Grains: As for Layer C1.12.

Mineralogy: 53% Aragonite, 20% calcite and 27% quartz.

Foraminifera: *Elphidium* (larger form), *Cibicides* (Open Marine) and *Ammonia beccarri*.

Mollusc Types: *Katelysia scalarina*, *Spisula (Notospisula) trigonella*, *Clanculus isoclanculus*, *Ostrea agassi* (tennis oyster), *Batillari diemensis* and *Tellina albinella*. Other unidentifiable fragments are also found.

Bryozoa: *Cellarid*-like branching form found.

Organic Analysis: Not performed.

XRD Carbonate Analysis: Not performed.

LAYER C1.14

Depth: **144.0 - 151.0cm**

Colour: Black.

Carbonate Grains And Other Components: Organic rich Layer with a sand size calcareous component. Some mollusc and echinoid fragments found.

Siliciclastic Grains: Very fine to fine, sub-angular to sub-rounded well sorted sand.

Mineralogy: 48% Aragonite, 23% calcite and 29% quartz.

Foraminifera: Not sampled.

Mollusc Types: Rare and only fragmented.

Organic Analysis: Sampled from 144.0 to 151.0cm (C1MM)

C.P.I	-	T_{max}	417	S1+S2	36.59
O.E.P (1)	-	T.O.C	23.89	P.I	0.31
Pr/Ph	-	H.I	106		
C25HBI/C31	-	O.I	164		

XRD Carbonate Analysis: Not performed.

LAYER C1.15 (Bottom Layer)

Depth: **151.0 - 160.0cm**
Colour: Grey.
Carbonate Grains And Other Components: Sand size calcareous component.
Siliciclastic Grains: Very fine to fine, sub-rounded to rounded well sorted sand.
Mineralogy: 45% Aragonite, 18% calcite and 37% quartz.
Foraminifera: Not sampled.
Mollusc Types: Rare.
Organic Analysis: Not performed
XRD Carbonate Analysis: Not performed.

CORE 2

LAYER C2.1 (Top Layer)
Depth: **0.0 - 48.8cm**
Colour: Green.
Carbonate Grains And Other Components: Calcareous mud. Small gastropods are present but rare. Appearance of a stromatolite-like structure from 0-3.0cm and 16.0-21.5cm. Death assemblage of gastropods from 21.5 to 24.0cm.
Siliciclastic Grains: Negligible
Mineralogy: 17% Aragonite, 80% calcite and 3% quartz.
Foraminifera: Not sampled.
Mollusc Types: *Coxiella striata.*
Organic Analysis: Not performed
XRD Carbonate Analysis: At 19.4cm depth detect (9.0 mol% $MgCO_3$) (HMC) and (2.5 mol% $MgCO_3$) calcite (LMC) compositions.
Cathodoluminescence: Done from 13.0 -15.8cm (C2.23) and from 39.8 - 48.6cm (C2.22).

LAYER C2.2
Depth: **48.8 - 51.0cm**
Colour: Green-brown.
Carbonate Grains And Other Components: Calcareous mud with rare gastropods
Siliciclastic Grains: Negligible.
Mineralogy: 32% Aragonite, 65% calcite and 3% quartz.
Foraminifera: Not sampled.
Mollusc Types: *Coxiella striata.*
Organic Analysis: Not performed.

XRD Carbonate Analysis: Not performed.
Cathodoluminescence: Not performed.

LAYER C2.3
Depth: **51.0 - 56.0cm**
Colour: Pink.
Carbonate Grains And Other Components: Calcareous mud with rare gastropods.
Siliciclastic Grains: Negligible.
Mineralogy: 13% Aragonite, 83% calcite and 4% quartz.
Foraminifera: Not sampled.
Mollusc Types: Rare *Coxiella.*
Organic Analysis: Not performed.
XRD Carbonate Analysis: Not performed.
Cathodoluminescence: Not performed.

LAYER C2.4
Depth: **56.6 - 59.9cm**
Colour: Green-brown.
Carbonate Grains And Other Components: Calcareous mud.
Siliciclastic Grains: Negligible.
Mineralogy: 39% Aragonite, 61% calcite and 0% quartz.
Foraminifera: Not sampled.
Mollusc Types: Not observed.
Organic Analysis: Not performed.
XRD Carbonate Analysis: Not performed.
Cathodoluminescence: Not performed.

LAYER C2.5
Depth: **59.9 - 61.7cm**
Colour: Pink..
Carbonate Grains And Other Components: Calcareous mud.
Siliciclastic Grains: Negligible.
Mineralogy: 0% Aragonite, 100% calcite and 0% quartz.
Foraminifera: Not sampled.
Mollusc Types: Not observed.
Organic Analysis: Not performed.

XRD Carbonate Analysis: Sample from 61.0cm is (9.5 mol% $MgCO_3$) calcite (HMC).
Cathodoluminescence: Not performed.

LAYER C2.6
Depth: **61.7 - 63.5cm**
Colour: Green-brown.
Carbonate Grains And Other Components: Calcareous mud.
Siliciclastic Grains: Negligible.
Mineralogy: 0% Aragonite, 100% calcite and 0% quartz.
Foraminifera: Not sampled.
Mollusc Types: Not observed.
Organic Analysis: Not performed.
XRD Carbonate Analysis: Not performed.
Cathodoluminescence: Not performed.

LAYER C2.7
Depth: **63.5 - 65.2cm**
Colour: Green-brown.
Carbonate Grains And Other Components: Calcareous mud.
Siliciclastic Grains: Negligible.
Mineralogy: 21% Aragonite, 78% calcite and 1% quartz.
Foraminifera: Not sampled.
Mollusc Types: Not observed.
Organic Analysis: Not performed.
XRD Carbonate Analysis: Sample from 64.0cm has (9 mol% $MgCO_3$) calcite (HMC).
Cathodoluminescence: Not performed.

LAYER C2.8
Depth: **65.2 - 67.5cm**
Colour: Pink.
Carbonate Grains And Other Components: Calcareous mud.
Siliciclastic Grains: Negligible.
Mineralogy: 10% Aragonite, 88% calcite and 2% quartz.
Foraminifera: Not sampled.
Mollusc Types: Not observed.
Organic Analysis: Not performed.

XRD Carbonate Analysis: Not performed.
Cathodoluminescence: Not performed.

LAYER C2.9
Depth: **67.5 - 69.2cm**
Colour: Green-brown.
Carbonate Grains And Other Components: Calcareous mud.
Siliciclastic Grains: Negligible.
Mineralogy: 21% Aragonite, 79% calcite and 0% quartz.
Foraminifera: Not sampled.
Mollusc Types: Not observed.
Organic Analysis: Not performed.
XRD Carbonate Analysis: Not performed.
Cathodoluminescence: Not performed.

LAYER C2.10
Depth: **69.2 - 71.9cm**
Colour: Pink.
Carbonate Grains And Other Components: Calcareous mud.
Siliciclastic Grains: Negligible.
Mineralogy: 27% Aragonite, 69% calcite and 4% quartz.
Foraminifera: Not sampled.
Mollusc Types: Not observed.
Organic Analysis: Not performed.
XRD Carbonate Analysis: Not performed.
Cathodoluminescence: Not performed.

LAYER C2.11
Depth: **71.9 - 74.0cm**
Colour: Green-brown.
Carbonate Grains And Other Components: Calcareous mud.
Siliciclastic Grains: Negligible.
Mineralogy: 21% Aragonite, 79% calcite and 0% quartz.
Foraminifera: Not sampled.
Mollusc Types: Not observed.
Organic Analysis: Not performed.
XRD Carbonate Analysis: Sample from 73.0cm has a (8 mol% $MgCO_3$) calcite (HMC) mineralogy.

Cathodoluminescence: Done from 72.9-75.5cm (C2.24) and includes Layer C2.12

LAYER C2.12

Depth: **74.0 - 76.1cm**

Colour: Bright pink.

Carbonate Grains And Other Components: Calcareous mud.

Siliciclastic Grains: Negligible.

Mineralogy: 8% Aragonite, 92% calcite and 0% quartz.

Foraminifera: Not sampled.

Mollusc Types: Not observed.

Organic Analysis: Not performed.

XRD Carbonate Analysis: Not performed.

Cathodoluminescence: Not performed.

LAYER C2.13

Depth: **76.1 - 83.6cm**

Colour: Colour is highly variable:

76.1 - 76.3 Dark Chocolate.

76.3 - 77.1 Pink.

77.1 - 78.1 Green-brown.

78.1 - 83.6 Green brown to chocolate brown.

Carbonate Grains And Other Components: Very organic rich calcareous mud..

Siliciclastic Grains: Negligible.

Mineralogy: 36% Aragonite, 64% calcite and 0% quartz.

Foraminifera: Not sampled.

Mollusc Types: Not observed.

Organic Analysis: Sampled from 76.0 to 83.0 cm (C2T).

C.P.I	-	T_{max}	431°C	S1+S2	167.01
O.E.P (1)	-	T.O.C	16.41	P.I	0.30
Pr/Ph	-	H.I	698		
C25HBI/C31	-	O.I	287		

XRD Carbonate Analysis: Not performed.

Cathodoluminescence: Not performed.

LAYER C2.14

Depth: **83.6 - 93.7cm**

Colour: Chocolate brown.

Carbonate Grains And Other Components: Very organic rich calcareous mud..
Siliciclastic Grains: Negligible.
Mineralogy: 37% Aragonite, 52% calcite and 11% quartz.
Foraminifera: Not sampled.
Mollusc Types: Not observed.
Organic Analysis: Not performed.
XRD Carbonate Analysis: Not performed.
Cathodoluminescence: Not performed.

LAYER C2.15
Depth: **93.7 - 96.5cm**
Colour: Brown.
Carbonate Grains And Other Components: Very organic rich calcareous mud..
Siliciclastic Grains: Negligible.
Mineralogy: 21% Aragonite, 78% calcite and 2% quartz.
Foraminifera: Not sampled.
Mollusc Types: Not observed.
Organic Analysis: Sample taken between 95.0 and 103.0 cm (C2.M), which includes units C2.16 C2.17 and C2.18.

C.P.I	5.65	T_{max}	426°C	S1+S2	167.01
O.E.P (1)	4.61	T.O.C	19.56	P.I	0.30
Pr/Ph	>>>1	H.I	595		
C25HBI/C31	0.57	O.I	287		

XRD Carbonate Analysis: Not performed.
Cathodoluminescence: Not performed.

LAYER C2.16
Depth: **96.5 - 98.7cm**
Colour: Chocolate brown.
Carbonate Grains And Other Components: Very organic rich calcareous mud.
Siliciclastic Grains: Negligible.
Mineralogy: 37% Aragonite, 46% calcite and 17% quartz.
Foraminifera: Not sampled.
Mollusc Types: Not observed.
Organic Analysis: See Layer C2.15.
XRD Carbonate Analysis: Sample from 98.0 gave two Mg-calcites. (12.5 mol% $MgCO_3$) and (4 mol% $MgCO_3$) calcite (HMC and LMC respectively).
Cathodoluminescence: Not performed.

LAYER C2.17

Depth: **98.7 - 99.3cm**

Colour: Cream.

Carbonate Grains And Other Components: Silt to mud grain size.

Siliciclastic Grains: Negligible.

Mineralogy: 34% Aragonite, 56% calcite and 10% quartz.

Foraminifera: Not sampled.

Mollusc Types: Not observed.

Organic Analysis: See Layer C2.15.

XRD Carbonate Analysis: Not performed

Cathodoluminescence: Not performed.

LAYER C2.18

Depth: **99.3 - 126.2cm**

Colour: Layered Layer:

99.3 - 104.0, Chocolate brown.

104.0 - 104.3 Cream.

104.3 - 126.2 Chocolate brown.

Carbonate Grains And Other Components: Cream coloured silt with darker (brown) mud.

Siliciclastic Grains: Negligible.

Mineralogy: 59% Aragonite, 38% calcite and 3% quartz.

Foraminifera: Not sampled.

Mollusc Types: Not observed.

Organic Analysis: Sampled between 115.0 and 128.4cm (C2.B), which includes Layer C2.19.

C.P.I	-	T_{max}	434°C	S1+S2	58.48
O.E.P (1)	-	T.O.C	8.58	P.I	0.37
Pr/Ph	-	H.I	433		
C25HBI/C31	-	O.I	224		

XRD Carbonate Analysis: Not performed.

Cathodoluminescence: Not performed.

LAYER C2.19 (Bottom Layer)

Depth: **126.2 - 128.4cm**

Colour: Khaki brown.

Carbonate Grains And Other Components: Calcareous mud. Appearance of stromatolite from 126.2 to127.2cm.

Siliciclastic Grains: Negligible.

Mineralogy: 77% Aragonite, 15% calcite and 8% quartz.

Foraminifera: Not sampled.

Mollusc Types: Not observed.

Organic Analysis: See C2.18.

XRD Carbonate Analysis: Sample from 128.0 cm has two calcite compositions, (13 mol% $MgCO_3$) calcite (HMC) and (3 mol% $MgCO_3$) calcite (LMC).

Cathodoluminescence: Not performed.

APPENDIX V

XRD RESULTS

A) Mineral Percentages
B) Trends

A. Condensed core XRD mineral percentages.

CORE 2

DEPTH(cm)	Aragonite%	Calcite%	Quartz%
6.5	16.3	80.1	3.6
19.4	22.8	73.7	3.5
41.2	11.6	85.3	3.1
49.8	32.4	64.7	2.9
54.1	13.1	83.1	3.8
58.3	38.5	61.5	0
60.8	0	100	0
62.8	0	100	0
64.4	20.7	77.9	1.4
66.6	10.1	87.9	2
68.6	20.8	79.2	0
70.7	26.8	69.4	3.8
73.1	21.4	78.6	0
75.2	8.3	91.7	0
79.5	36.1	63.9	0
87.9	37	52.1	10.9
95.3	20.6	76.7	2.7
97.9	36.9	46	17.1
99.1	33.5	56.2	10.3
111.8	58.5	37.8	3.7
127.7	77.1	15.4	7.5

CORE 3

DEPTH(cm)	Aragonite%	Calcite%	Quartz%
3	52.2	44.2	3.6
13.7	29.6	65.1	5.3
27.6	44.6	54.1	1.3
34.3	14.6	83.2	2.2
38.4	18.7	78.4	2.9
42.2	13.3	82.9	3.8
44.2	11.9	81	7.1
48.7	30.4	51.4	18.2
52.6	79.7	17.7	2.6
63	40	14	46
88.5	32.6	19.6	47.8
110.5	53.8	13.7	32.5
132.7	62	10.7	27.3

CORE 4

DEPTH(cm)	Aragonite%	Calcite%	Quartz%
3.9	68.4	27.1	4.5
14.7	15	82.7	2.3
23.5	17.8	79.4	2.8
28.4	25	54.3	20.7
36	20.7	75.9	3.4
45.5	56.3	35.8	7.9
64.7	56.9	19	24.1
88.2	53.2	19.7	27.1
98.7	47.6	22.6	29.8
134.6	44.9	18.3	36.8
169.8	11	80.3	8.7
177.4	0	0	100
185.2	43.5	3.4	53.1

CORE 5

DEPTH(cm)	Aragonite%	Calcite%	Quartz%
5	52.1	43.7	4.2
16.4	21.3	77.3	1.4
19.9	24.7	73.9	1.4
22.2	25.2	61.9	12.9
25.9	31	62	7
29	23.3	69.3	7.4
31.9	10.4	77.8	11.8
36.6	21.1	76.1	2.8
42.5	32.6	59.8	7.6
52.1	20.9	68.4	10.7
61.2	87.7	9.3	3
71.9	58.9	9.6	31.5
84.8	55.6	13.1	31.3
105.5	56.6	13.9	29.5
124.5	44.3	23.8	31.9
140.4	52.1	15.2	32.7
159.8	30.4	20.9	48.7

B. XRD Mineral trends with depth for cores C2,C3,C4 and C5. (Condensed Cores)

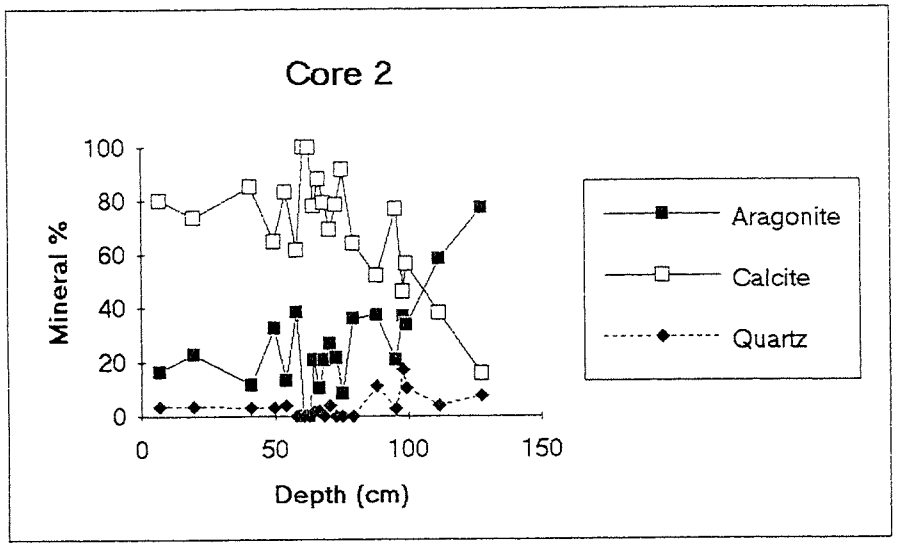

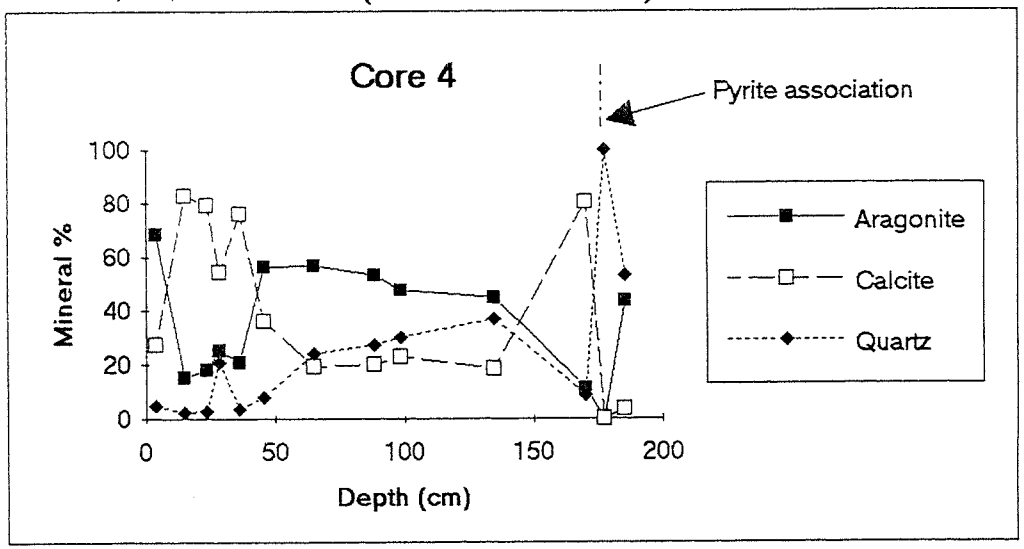

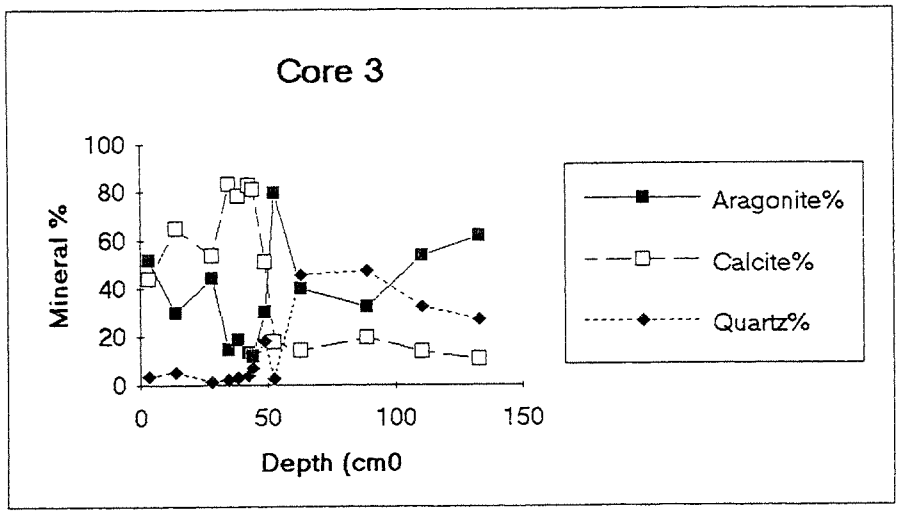

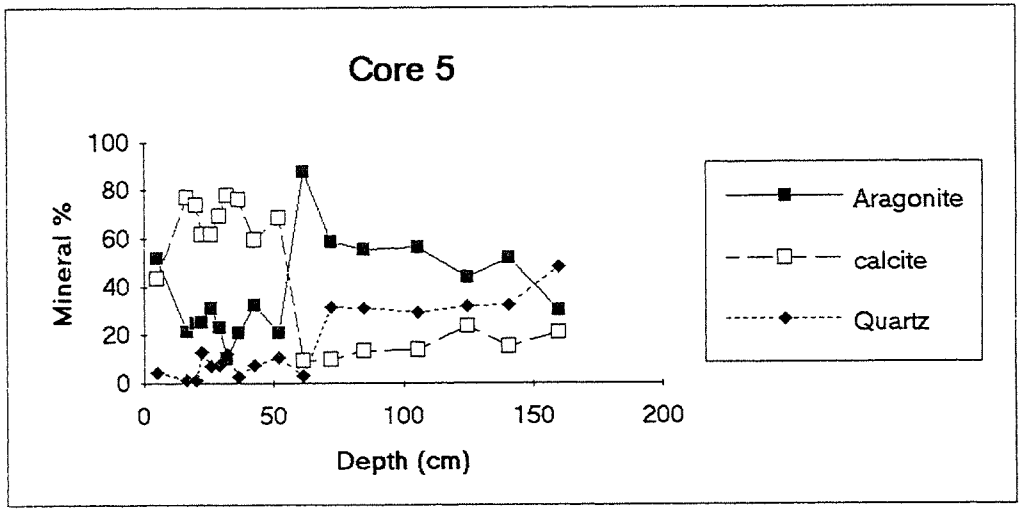

APPENDIX VI

VAN KREVELEN DIAGRAMS

HYDROGEN INDEX vs T max

Client: UNIVERSITY OF ADELAIDE
Location: OLD MAN LAKE

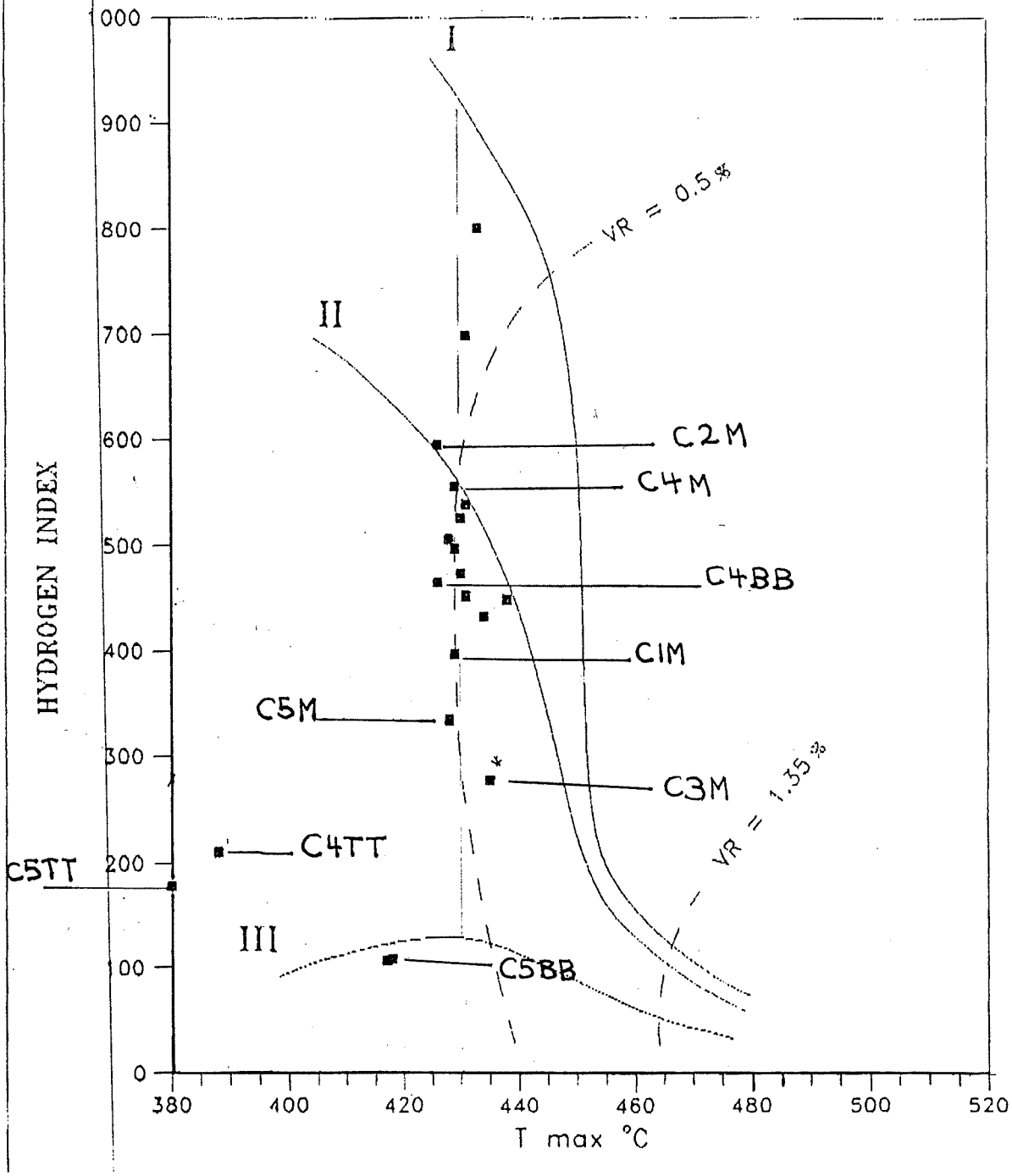

KEROGEN TYPE

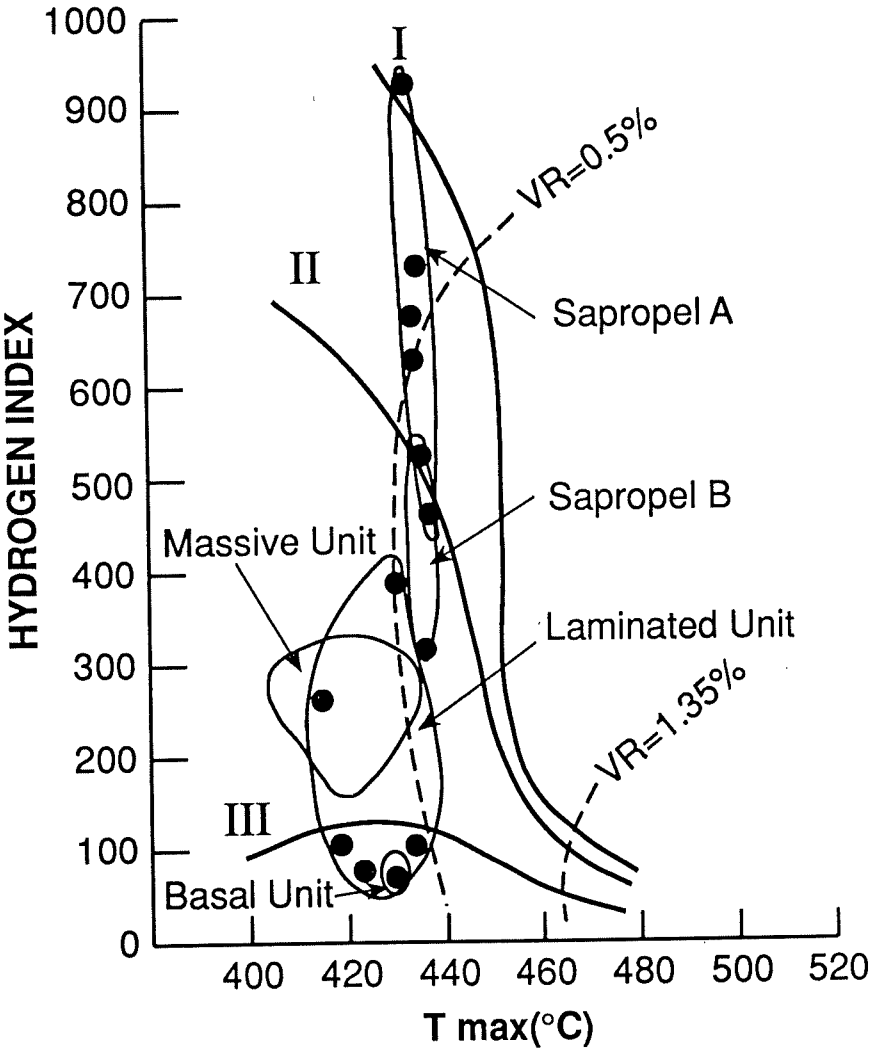

(After Hayball et al 1993)